HHS Public Access

Author manuscript

ACS Nano. Author manuscript; available in PMC 2017 April 26.

Published in final edited form as:

ACS Nano. 2016 April 26; 10(4): 3918–3935. doi:10.1021/acsnano.6b01401.

Scintillating Nanoparticles as Energy Mediators for Enhanced Photodynamic Therapy

Anyanee Kamkaew[1], **Feng Chen**[1,*], **Yonghua Zhan**[1,2], **Rebecca L. Majewski**[3], and **Weibo Cai**[1,4,5,*]

[1]Department of Radiology, University of Wisconsin - Madison, Wisconsin 53705, United States

[2]Engineering Research Center of Molecular and Neuro Imaging of the Ministry of Education & School of Life Science and Technology, Xidian University, Xi'an, Shaanxi 710071, China

[3]Department of Biomedical Engineering, University of Wisconsin - Madison, Wisconsin 53705, United States

[4]Department of Medical Physics, University of Wisconsin - Madison, Wisconsin 53705, United States

[5]University of Wisconsin Carbone Cancer Center, Madison, Wisconsin 53705, United States

Abstract

Achieving effective treatment of deep-seated tumors is a major challenge for traditional photodynamic therapy (PDT) due to difficulties in delivering light into the sub-surface. Thanks to its great tissue penetration, X-rays hold the potential to become an ideal excitation source for activating photosensitizers (PS) that accumulate in deep tumor tissue. Recently, a wide variety of nanoparticles have been developed for this purpose. The nanoparticles are not only designed as carriers for loading various kinds of PSs, but also can facilitate the activation process by transferring energy harvested from X-ray irradiation to the loaded PS. In this review, we focus on recent developments of nanoscintillators with high energy transfer efficiency, their rational designs, as well as potential applications in next generation PDT. Treatment of deep-seated tumors by using radioisotopes as an internal light source will also be discussed.

Graphical abstract

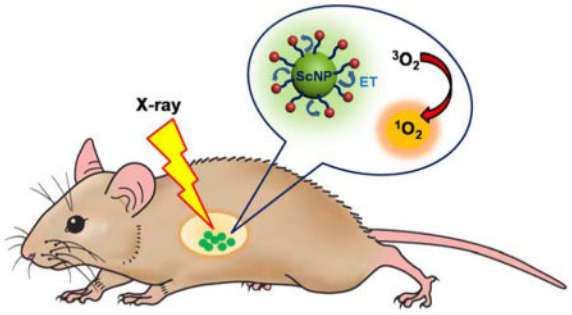

Corresponding Author: Feng Chen: fchen@uwhealth.org; Weibo Cai: wcai@uwhealth.org.

Keywords

Scintillating nanoparticles; Photodynamic therapy; X-ray activatable nanoparticles; Photosensitizer; Radiosensitizer; Cerenkov radiation; Cancer therapy; Energy mediator; Scintillator

Photodynamic therapy (PDT) is a noninvasive technique that is approved for the treatment of carcinoma.[1] In PDT, a photosensitizer (PS) is activated by a specific wavelength of light to generate reactive oxygen species (ROS), including singlet oxygen ($^1O_2$), which is considered a major toxic agent.[2, 3] To make PDT most effective, the light must be efficiently delivered to the PS. Lasers and light-emitting diodes (LEDs) are light sources that are commonly used in PDT, though in some cases halogen and arc lamps can also be used. However, most PSs, such as porphyrin derivatives, absorb in the ultraviolet or visible regions which overlap with the tissue absorption spectrum.[4, 5] This makes it difficult to apply PDT in the clinic due to the short penetration depth of illumination light, which leads to ineffective treatment of tumors located deep under the skin.

A potential solution to the limitation of PDT for deep tumor treatment is developing near-infrared (NIR) photosensitizers. Due to the weak scattering and absorption of most tissue chromophores, including oxyhemoglobin, deoxyhemoglobin, melanin, and fat in the NIR window, only light in the range of 700–1100 nm can penetrate deep into the tissue.[6] Unfortunately, one of the major challenges in the field is finding a suitable PS that can absorb light with a wavelength longer than 700 nm. Current PSs that have been extensively studied are phthalocyanine dye, which has a maximum absorption around 650–700 nm, and heptamethine dye, which has a maximum absorption around 650–850 nm.[7, 8] However, for practical applications, NIR light can still only penetrate 5 mm into the tissue since enough energy needs to be reserved for PS activation.[9] Moreover, reduced $^1O_2$ generation efficiency has been reported by using NIR-activated PSs due to the narrow energy gaps and the faster non-radiative transition rate (when compared with that of wide-band photosensitizers).[10, 11]

The growth of nanotechnology in the fields of biology and medicine presents versatile opportunities to overcome the limitations associated with the traditional strategies of PDT by combining multiple approaches in a unified one-piece therapeutic strategy.[12, 13] A current strategy that has been widely explored is using nanoparticles (NPs) as PS carriers to improve passive and active targeting ability.[14–17] For passive targeting, NPs tend to have long circulation times and concentrate more in tumor evironments compared to normal tissues due to the enhanced permeability and retention (EPR) effect.[18, 19] For active targeting, the surface of NPs can contain modified various targeting ligands, such as an antibody or antibody fragments, that recognize specific surface receptors on tumor cells to enhance the uptake of the NPs. [20–25] Therefore, the use of NPs is promising to improve the therapeutic efficacy in deep tissue. For example, upconversion nanoparticles (UCNPs) that can be excited by NIR light (*e.g.* 980 nm) and emit UV–visible (Vis) light have been reported for activating PSs for an enhanced therapeutic efficacy.[14, 26, 27] Another methodology used to achieve deeper tissue penetration is through utilizing an NIR laser as the light source. Even with this advancement there is still room for further improvement of the penetration depth and the generation efficacy of $^1O_2$.[28]

To work on overcoming these problems, researchers introduced X-rays as an energy source to initiate PDT.[29] The utilization of X-rays as a PDT light source makes it feasible to integrate diagnosis, radiotherapy, and PDT for the next generation of tumor theranostic applications. In order to use X-rays in this technology, scintillator materials are used to convert the X-rays to UV/visible light, since there is no PS that can directly absorb X-ray energy.[30] The scintillation process can be divided into three parts: (i) conversion of incoming radiation into a large number of electron-hole pairs, (ii) transfer of the electron-hole pairs' energy to the luminescent ions, and (iii) emission of the luminescent ions that radiatively return from an excited state to the ground state.[30, 31]

Herein, we diccuss the latest advancements in treating deep-seated tumors by PDT-based strategies using scintillating nanoparticles (ScNPs) as energy mediators. In addition to discussing various types of ScNPs, current PDT strategies are reviewed. These strategies are classified based upon the excitation energy source and the radionucleides used in the methodology.

A Brief Introduction of X-ray Technology

X-ray techniques were discovered in 1895 by Wilhelm Röntgen, a German physicist, and have since been used for non-invasive high-resolution medical imaging. In the 20th century and beyond, many X-ray applications have gained more attention, particularly for medical purposes. This is partially due to the fact that X-ray related imaging equipment became more sophisticated to improve visualization for biochemistry and disease pathology applications.

For these applications, it is useful to understand that different energy ranges are utilized for distinctive cancer targets. Low-energy beams (40–100 kV, kilovoltage or "superficial" X-rays) are useful only for skin cancers since the beams can only penetrate <5 mm in depth. Sub-surface tumors require medium energies (200 kV to 1 MV orthovoltage and supervoltage X-rays). Presently, high-energy beams (4–25 megavoltage [MV] or "deep" X-rays) are commonly used to treat deep tumors (> 2 cm in depth). The International System of Units (SI) derived unit for absorbed dose is the gray (Gy), equivalent to one joule of energy deposited by ionizing radiation per kilogram of matter (1 Gy = 1 J/kg = 1 m^2/s^2).[32, 33]

Heavy Elements Enhance Radiation Effects

Heavy elements are known to have high potential to be radiosensitizers.[34] For example, Cisplatin, a platinum-containing DNA-crosslinking drug, was demonstrated to enhance the effects of ionizing radiation through the "high Z effect," known as Auger therapy.[35] In the case of X-ray irradiation, the photoabsorption cross-sections of inner-shell electrons are much larger than those of the outer shell electrons, and high-Z elements have larger total photoabsorption compared to low-Z atoms.[36] Furthermore, heavy atoms have considerably higher photoelectric cross-sections than soft tissue for sub-MeV energies. This photoelectric effect is defined by $(Z/E)^3$ where $E = h\nu$ is the incoming photon energy and Z is the atomic number of the targeted molecule.

The photoelectric effect can be observed when metals emit electrons, also called photoelectrons, once light shines upon them. When ionized by X-ray or γ-ray energy, mid-

to high-Z elements can produce a cascade of low-energy Auger electrons that can locally enhance the effective radiation dose. Another method to provide radiation dose enhancement is to use dense inorganic nanoparticles. The enhancement then depends on the composition and size of the particles, uptake of particles into cells, and the energy of the applied radiation. Scheme 1 shows the possible outcomes that occur when X-rays interact with metal. Among these, scattered X-rays/photons, photoelectrons, Compton electrons, Auger electrons, and fluorescence photons are the most relevant to cancer radiotherapy. It is also worthy to mention that fluorescent emissions from atoms hit by X-rays can be beneficial for molecular imaging and PDT purposes.

Spatial resolution is an important characteristic for molecular imaging modalities and should be addressed as it pertains to X-rays. Spatial resolution refers to the minimum distance where the imaging modality can differentiate two independently measured objects.[37] The lower the spatial resolution, the more details can be obtained from the resulting image. For example, optical imaging is a highly sensitive technique but does not offer good spatial resolution except for super-resolution imaging techniques, where spatial resolution can be improved to 10 nm.[38] However, super-resolution imaging techniques are still not widely used in clinical applications. In comparison, X-ray imaging has recently been developed to offer very high spatial resolution (sub-30 nm)[39–41] which is useful for many medical applications.[42–45]

X-ray Sensitive Nanoprobes for Biomedical Imaging

X-ray computed tomography (CT) is widely used to image anatomy with high spatial resolution, but its sensitivity is not high enough to use in molecular imaging.[46] However, in the past decade, X-ray luminescence imaging has been proposed as an imaging modality for biological imaging applications.[47–49] This has been proposed partially due to the recent development of phosphor nanoparticles (PNPs), which opens possibilities to utilize X-rays for molecular imaging purposes *in vivo*. PNPs that luminesce NIR light upon becoming excited *via* X-ray photons have been developed for imaging.[50, 51] The distinct combination of the high sensitivity radioluminescent nanoparticles and the high spatial localization of collimated X-ray beams make this technique even more useful in molecular imaging.

In X-ray imaging, X-ray luminescence computed tomography (XLCT) and X-ray fluorescence computed tomography (XFCT) are two emerging technologies that provide functional and molecular imaging capabilities.[47] Both modalities use external X-rays to stimulate secondary emissions, either in the form of light or secondary X-rays, which are acquired for tomographic reconstruction. These modalities exceed the current sensitivity of present X-ray imaging technologies, leading to the potential of utilizing X-rays to reveal molecular imaging information. Moreover, these integrations break through the spatial resolution limits of other *in vivo* molecular imaging modalities.[48, 49, 52]

Polymer dots (P-dots) are considered a class of fluorescent, organic NPs for biological imaging.[53] In addition, Iridium(III) complexes are one the most promising compounds for plastic scintillators since Ir(III) has high electron density with an atomic number of 77.[54] To utilize the benefits of both technologies, Ir(III) complex-doped P-dots were synthesized, and their X-ray luminescence abilities were evaluated.[55] Luminescence from Ir(III) complex-

doped P-dots was observed upon X-ray irradiation (50 kVp and 30 mA) leading to potential use in XLCT imaging. Two possible mechanisms of X-ray induced emission have been proposed: direct and indirect excitation of the Ir(III) complex. For direct activation, the complex was excited *via* X-ray beams then emitted visible light. For the indirect mechanism, a combination of excitons formed in P-dots generated a triplet excited state of the polymers, and after receiving a photon from the X-rays, the energy was transferred to the Ir(III) complex to emit light. However, more physical and biological studies need to be conducted in order to confirm the mechanism hypothesis, examine toxicity, and further support the effectiveness of this system.

Lanthanide-doped nanoparticles have a high atomic number and proper electronic energy states. They can emit photons in the UV, visible, and NIR regions, and have been considered to be a suitable choice for scintillating materials since they emit visible photons when irradiated with γ- or X-rays.[56] Great efforts have been devoted to developing nanophosphors for X-ray luminescence optical tomography (XLOT) applications.[57–59] Recently, $NaGdF_4$-doped Eu^{3+} nanoparticles were synthesized and studied systematically for applications in X-ray excited luminescence.[60] The Gd^{3+}–Eu^{3+} host–dopant combination is considered to be the best combination for a down-conversion system because the emission energy transitions within Gd^{3+} can resonantly couple to the excited state of Eu^{3+} ions. Among nanomaterials that have been reported so far, $NaGdF_4$:Eu^{3+} NPs claim to be the most efficient X-ray excited luminescence phosphor.[60] The $NaGdF_4$:Eu^{3+} NPs were synthesized by the citrate method,[61] and the crystal structure was found to be both hexagonal and cubic, measuring 30 nm in size. Upon X-ray irradiation, the hexagonal phase showed two times stronger luminescence than the cubic phase and the emission intensity was found to be pH dependent, which is a unique effect that has not been seen before with UV excitation. Although coating NPs with a gold layer affected the overall emission, it did not affect the most important $^5D_0 \rightarrow {}^7F_4$ NIR line (692 nm) emission, maintaining the ability of the gold-coated nanoscintillator to be used for XLOT.

Another interesting study is to use X-ray sensitive NPs to monitor drug release in the target cells, which was completed using Gd_2O_2S:Tb radioluminescent nanocapsules. In this study, the nanocapsules were used for carrying a hydrophilic drug, Doxorubicin (DOX), while the release kinetics of the drug were also monitored.[62] Transmission electron microscopy (TEM) images showed the average length of the capsules to be 420 ± 20 nm with a width of 130 nm ± 15 nm. Styrenesulfonate sodium (PSS) and poly(allylamine hydrochloride) (PAH) were decorated on the nanocapsules as polyelectrolytes in the pH-controlled release systems. Upon X-ray excitation, the luminescence spectrum changed during the release of the optically absorbing DOX chemotherapy drug. The release rate could be monitored *in situ* by tracking the ratio of radioluminescence spectral peaks. The use of this nanosystem was further demonstrated *in vivo*. Furthermore, a maximum tolerated dose study indicated no morbidity or weight loss was observed at doses up to 400 mg/kg. This technique is advantageous over the other optical techniques that used external excitation sources because the X-rays can penetrate deeper in the tissue. Thus, tissue absorption and scattering will not interfere with the luminescence signal.

X-ray excitation of other luminescent nanomaterials, such as metal–organic frameworks,[63] gold nanoclusters,[59] and radioluminescent nanophosphors,[64] has also been studied. However, most generated emission spectra were similar to the traditional optical excitation with high tissue autofluorescence background. The development of X-ray excitable nanoprobes with bright near-infrared luminescence could provide a solution to this problem. For example, X-ray activatable rare-earth doped nanoprobes (REs) have recently shown great promise for shortwave infrared (SWIR or NIR-II, NIR window range 1000–2300 nm) molecular imaging.[65] $NaYF_4$ nanoparticles were doped with two different rare-earth elements, ytterbium (Yb) and erbium (Er). Both Yb and Er doping play important roles in SWIR emission. Under X-ray excitation, $NaYF_4$: Er,Yb showed characteristic SWIR emissions peaking at 1532 nm (observed by SWIR detector). Biodistribution studies showed most of this material was accumulated in the liver, with some in the spleen and the lungs, due to their large size and possible aggregation *in vivo*. Also, the PEG-modified NPs were capable of X-ray-induced SWIR luminescence (X-IR) imaging for mapping lymphatic drainage at resolutions that are sufficient to identify individual nodes (Figure 1).

X-ray Induced Photodynamic Therapy

To overcome the limitation of tissue-penetration depth in traditional PDT, researchers introduced X-ray as a promising light source that can deliver light to the hidden tissue. However, no conventional photosensitizer can directly absorb X-ray radiation for generating $^1O_2$. Over the past few years, nanoparticles have been developed to not only be the carriers for photosensitizers, but also act as energy transducers.[12, 13] The combination of radiation therapy and PDT could potentially provide an improved therapeutic outcome for deep-seated cancer.

Principle of X-ray Activatable Nanoparticles for PDT

The principle of X-ray activatable nanoparticles for PDT is presented in Scheme 2. After the nanosensitizer systems have accumulated at the tumor site, X-rays will be given to stimulate the encapsulated metal to generate emission light. The emission light can then be harvested for activating the nearby PS for X-ray induced PDT. Wide band-gap materials are employed for the transformation of the X-rays to UV/visible photons. The conversion of X-ray energy occurs within 1 ps. A cascade interaction of high energy photons with the ScNP's lattice occurs through the photoelectric effect and the Compton scattering effect, in which many electron–hole pairs are created and thermalized in the conduction and valence bands, respectively. Subsequently, electrons and holes, which eventually create excitons, migrate through the material. Repeated trapping at defects in the material may occur, and energy losses are probable due to nonradiative recombination as well as other mechanisms. The recapture of the charge carrier in the material forbidden gap can introduce considerable delay in the migration. This recapturing stage is the least predictable as material point defects, flaws, surfaces, and interfaces can introduce energy levels into the forbidden gap and strongly modify or degrade otherwise high intrinsic scintillation performance. The final stage, luminescence, consists of consecutive trapping of the electron and hole at the luminescence center followed by their radiative recombination. [30, 31] At the same time, the

luminescence (energy) from the ScNPs will activate the nearby PS leading to $^1O_2$ generation, which is very toxic to the cells.

In PDT, there are two types of reactions that occur after the PS absorbs energy.[66] Electrons from the ground state (S_0) are transformed to singlet-excited states (S_1). Some of the absorbed energy will be released *via* intersystem crossing (ISC), and the promoted electron will move to a triplet-excited state (T_1), which has a relatively long half-life. Then, this excited triplet electron can undergo two kinds of reactions (Scheme 2b). In the type I pathway, the electron directly reacts with a substrate, *i.e.* cell membrane or a molecule, to form radicals that can interact with oxygen to produce reactive oxygen species (ROS), such as hydrogen peroxide (H_2O_2), hydroxyl radicals (·OH), and oxygen radicals ($\cdot O_2$). Alternatively, in the type II pathway, the triplet electron directly transfers the energy to triplet oxygen ($^3O_2$) nearby to form a highly ROS ($^1O_2$). Both Type I and Type II reactions can occur simultaneously, and the ratio between these processes depends on the type of PS used and the concentrations of substrate and oxygen; however, in most cases the PDT often occurs *via* the type II pathway. Moreover, PDT is only effective in a proximal area of ROS production since $^1O_2$ has a very short half-life in biological systems (< 40 ns).[67]

Currently, there are some PSs that have good clinical outcomes in oncology, and many of these are commercially available.[68] Porfimer sodium (Photofrin®) is a hematoporphyrin derivative known as the earliest clinical PDT agent. This agent is available from Axcan Pharma and has been approved for treatment of several diseases, including cancers of the esophagus, lung and bladder. Although this PDT agent can be activated at 630 nm, it requires extended irradiation from a high-energy source, which often leads to complications. Another disadvantage of Photofrin® is that it is not cleared quickly, leading to post-treatment skin photosensitivity.[69] Most porphyrin derivatives can be activated by using red light (~630–680 nm), but photons of this wavelength do not penetrate tissue beyond a few millimeters. Therefore, this type of PS is only suitable for superficial tumors, or tumors that can be reached *via* endoscopic or fiber optic procedures. Consequently, many researchers have developed nanomaterials that can convert high energy photons to UV/visible light that can activate porphyrins at the strong absorption band (~ 400 nm).

General Photosensitizer Loading Strategies

Porous Silica Encapsulation—Mesoporous silica nanoparticles (MSNs) are widly used as nanocarriers for drug delivery[70] due to their intrinsic porous structure and outstanding biocompatibility, which are both beneficial for PS loading. Due to its porous nature, MSN coatings have also been found to have a superior efficiency of energy transfer.[14] Moreover, the large surface area of MSN also facilitates the multiple PS loading for enhanced PDT. However, this technique is more suitable for cationic, hydrophilic PS loading due to the negatively charged silica matrix (Scheme 3). Unfortunately, there is also a high chance of hydrophilic PS leakage out of the uncapped pores during systemic circulation, which could lead to undesired phototoxicity.

Physical Loading—Physical loading of PSs to NPs can be achieved based on either electrostatic adherence[71] or hydrophobic interaction.[72, 73] The electrostatic adherence

method is accomplished through utilizing the interactions between opposing charged components, such as charged nanoparticles and ionized PSs. However, this approach requires tedious modification processes which usually result in an unexpected decrease in $^1O_2$ generation and quantum yield. A more efficient way of physical loading is utilizing hydrophobic interactions between NPs and PSs. In general, NPs are coated in oil solvents containing hydrophobic alkane chains (such as oleic acid or trioctylphosphine oxide), then wrapped in an aqueous phase with hydrophilic polymers such as polyethylenimine (PEI), polyethylene glycol (PEG), chitosan, cyclodextrin, or tween-20. A hydrophobic layer is created beneath the hydrophilic surface to adsorb PSs on the NPs *via* a hydrophobic interaction, leaving the outer shell for water solubility purposes (Scheme 3). This method allows for a high PS loading capacity and keeps the PS in close proximity with the NPs to ensure efficient energy transfer. However, too much PS loading does not always guarantee a better PDT performance since the high PS concentrations could form aggregations or dimers (which usually generate much less or no $^1O_2$).[74]

Covalent Conjugation—Due to the complicated physiological microenvironment *in vivo*, nanocomposites fabricated with the abovementioned approaches usually cannot retain their stability for *in vivo* applications. To overcome this, a covalent conjugation strategy was proposed. Chemical linkage or covalent conjugation requires the PS to be chemically attached to the NPs surface to avoid the PS's pre-release and off-targeting issues. PSs with active functional groups such as carboxyl groups (-COOH), amino groups (-NH_2), or sulfhydryl groups (-SH) can be linked to NP surfaces under certain conditions. Often, an amide coupling reaction is used to conjugate the carboxyl group on the PS to the amine on the NPs (Scheme 3). In addition to being used for the conjugation of the PS, the amino group on NPs allows for the attachment of other targeting moieties such as antibodies, peptides, or small molecules for tumor selectivity. This approach is beneficial in that it offers higher selectivity, more control over PS loading, and control over the distance between the NPs and PS molecule. However, its application is limited to *in vitro* studies because the PS payload achieved using covalent linkages was usually relatively small.

Direct Surface Coating—For optimum and reproducible therapeutic efficiency, it is essential to design a controllable and robust PS coating system. Inorganic PSs such as ZnO or TiO_2 can be directly coated on the NPs surface (Scheme 3) for PDT applications.[75–78] These nanoconstructs allow for controllable and uniform PS loading on individual NPs and significantly reduce the possibility of PS leakage with greatly enhanced ROS generation.

In general, nanoparticles that are capable of X-ray induced PDT must meet certain requirements. First, good overlapping of the NP emission spectra with the PS's absorption profile is required to ensure the activation efficiency of PS and $^1O_2$ production. This can be achieved by using suitable doping strategies as well as controlling the NP size. Second, NPs should have a high luminescence efficacy once they are irradiated by X-ray or other radiation forms. Moreover, the NPs must be synthetically accessible and easily attached to PSs. Finally, the nanosystem must be water-soluble, non-toxic, and stable in biological environments.

Rare Earth Elements-Based Nanoparticles

Conventional radiation therapy combats cancer by using high doses of radiation to damage cancer cells, which is also harmful to normal cells due to the non-targeted nature of the therapy. The integration of conventional radiation therapy with PDT could potentially achieve a better outcome by lowering the necessary radiation doses. To begin to achieve this goal, X-ray activatable NPs were first reported by Chen and co-workers in 2006.[29] The authors used scintillating NPs to deliver PSs (*i.e.* porphyrins) to the treatment site *in vivo.* The NPs transduced the absorbed X-ray light to activate the PSs, resulting in the production of $^1O_2$ for killing the cancer cells. Rare earth elements-based nanoparticles, such as BaFBr:Eu^{2+}, BaFBr:Mn^{2+}, LaF_3:Ce^{3+}, and LaF_3:Tb^{3+}, have been reported to persistently luminescence when exposed to X-rays.[79] Interestingly, at a higher ambient temperature, *i.e. in vivo*, the “afterglow” period (the period of persistent luminescence) is increased.

Porphyrins are known to have a strong absorption peak at around 400 nm (termed the Soret band) and other weak absorption peaks at around 600–800 (termed the Q-band). Thus, excitation at the Soret band would give much higher efficiency in $^1O_2$ generation. However, excitation in the UV/blue light range limits the clinical application of PDT as this light has much shorter penetration depth in tissues when compared with red light. In order for excitation to occur at the stronger absorbing Soret band of porphyrins, scintillating NPs were used as an internal energy source. These NPs can emit luminescence in the visible region (peaking at 400, 500 and 650 nm) upon exposure to X-rays, making it possible for the porphyrins to be activated at both the Soret band and Q-band for even more efficient PDT.[29, 79]

For example, fluorescence quenching techniques were used to demonstrate the energy transfer process of hydrophilic LaF_3:Tb^{3+} NPs to the conjugated meso-tetra(4-carboxyphenyl)porphyrin (mTCP) upon X-ray irradiation.[80] The results showed the LaF_3:Tb^{3+}-mTCP nanocomposites could be activated by X-rays at a reasonably lower dose (250 keV, 0.44 G/min for 30 min) than the regular radiation therapy (high energy X-rays with MeV energies are used).[81] In an attempt to improve cancer targeting, the LaF_3:Tb^{3+}-mTCP system was conjugated to folic acid, and the results confirmed that folic acid conjugation NPs had no effect on $^1O_2$ generation. Neither *in vitro* nor *in vivo* studies of this system have been reported so far.

In another study, Ce^{3+}-doped lanthanum(III) fluoride (LaF_3:Ce^{3+}) NPs were encapsulated in poly-lactic-co-glycolic acid (PLGA) microspheres along with protoporphyrin IX (PPIX).[73] Under X-ray irradiation (90 kV), energy was transferred from the LaF_3:Ce^{3+}/DMSO NPs to the PPIX producing $^1O_2$ that damaged prostate cancer cells (PC-3). The LaF_3:Ce^{3+}/DMSO NPs were found to have a strong emission peak at approximately 520 nm that overlapped well with one of the weak absorption bands of PPIX. However, the Soret band was not excited in this system.

Lanthanide-doped fluoride/oxide nanoparticles such as LaF_3:Tb^{3+}/Ce^{3+} or Tb_2O_3 are often used as X-ray energy acceptors. Although the amount of $^1O_2$ produced by scintillating NP-PS systems upon X-ray irradiation is several times higher than the amount from PSs alone, X-ray excited PDT is still not as efficient as conventional PDT. One potential mechanism

could be because the effectiveness of PDT relies on efficient energy transfer, where better spectrum overlapping usually shows an improved PDT effect. Moreover, the post-modification processes could compromise the PDT efficacy.

Mesoporous LaF_3:Tb^{3+} ScNPs encapsulated with a water-soluble PS (Rose Bengal [RB]) were prepared to enhance the Förster Resonance Energy Transfer (FRET) process.[82] The NPs were prepared by a facile hydrothermal process without using a catalyst, surfactant, or template. The optimized NPs can emit strong green luminescence under both UV light and X-ray excitation. RB was simply attached to the nanosystem *via* a pore loading strategy (Figure 2a and 2b), which holds several advantages, including (i) a well definite nanostructure, (ii) spectrum overlap between the NP's emission band at 544 nm and RB's major absorption at 549 nm (Figure 2d), (iii) optimized scintillating luminescence, (iv) a simple drug loading approach, (v) high FRET efficiency, (vi) good water solubility, and (vii) ultra-colloidal stability. The ratio of Tb^{3+} doping affected luminescence intensity at 544 nm under UV and X-ray stimulation of the mesoporous LaF_3:Tb^{3+} ScNPs (Figure 2c). Energy transfer efficiency was found to be as high as 85%, which was analyzed by steady state spectra and fluorescence delay dynamic analysis. $^1O_2$ generation from these ScNPs was also enhanced when compared to free RB (Figure 2e).

In another study, multifunctional LaF_3:Tb^{3+}-RB nanoscintillations were coated with homogenous layers of silica with a tunable shell thickness and covalently bound with Rose Bengal for tumor diagnosis. [83] The nanocomposites had a uniform size, high colloidal stability, high luminescence efficiency, photostability, and biocompatibility. Furthermore, the X-ray attenuation ability was measured and *in vivo* X-ray imaging was performed on a tumor-bearing mouse. The signal intensity in the tumor was found to be greatly enhanced after intratumor injection. The X-ray attenuation power was determined to be better than the clinical CT contrast agent, Ultravist® 300, which makes the nanoscintillations an ideal contrast agent to be engaged in deep-seated tumor diagnosis (CT imaging) and therapy (PDT). Although promising, more studies are needed to further validate the PDT effects of LaF_3:Tb^{3+}-RB nanoscintillating system under X-ray irradiation.

Gadolinium oxysulfide doped with terbium (*i.e.* Gd_2O_2S:Tb, size: ~20 microns) was reported as an indirect activator of Photofrin II (Photo II) upon X-ray excitation.[84] The Gd_2O_2S:Tb phosphor has been widely used in radiographic intensifying screens (scintillating screens) in medical imaging systems, such as X-ray fluoroscopy, X-ray Computed Tomography (X-CT), Single Photon Emission Computed Tomography (SPECT), and Positron Emission Tomography (PET), due to its high absorption of X-ray energy and high conversion efficiency into visible light.[85] In one study, the nanoscintillating system was co-incubated with Photo II to study its PDT effect upon X-ray irradiation *in vitro*. By using 120 kVp diagnostic X-rays, metabolic activities of human glioblastoma cells were found to be suppressed dramatically. Interestingly, the NPs alone (without Photofrin) protected the cells against X-ray irradiation. Since the NPs did not covalently conjugate with PS, the energy transfer efficiency could be restricted. An enhanced PDT efficacy could be expected when conjugating Photofrin II to the surface of Gd_2O_2S:Tb NPs to minimize the energy transfer distance. Unfortunately, *in vivo* X-ray induced PDT data has yet to be reported.

Terbium oxide (Tb_2O_3) nanoparticles are also widely used as scintillating NPs. Tb_2O_3 coated with a polysiloxane layer (Tb_2O_3@SiO_2) is known to be a biocompatible nanoscintillator.[86] Gd-free Tb_2O_3 has been found to have a higher density (8.230 g·cm^{-3}) as compared to Gd_2O_3:Tb (7.901 g·cm^{-3}), and it has also been found that luminescence quantum yield was preserved even if the NPs are small in size (inner core diameter ~3 nm). Since the biological and chemical properties of Tb_2O_3 are well established, it was interesting to study the physical characteristics of this nanosystem when combined with a photosensitizer, 5-(4-carboxyphenyl)-10,15,20-triphenyl porphyrin (TPP), in order to offer proof for the concept of X-ray activated PDT. The energy transfer mechanisms were demonstrated under UV excitation (Scheme 4a). The TPP fluorescence decay curve showed two components, fast and slow. The fast component corresponded to a direct excitation of TPP by laser, and the slow component was from Tb^{3+} transferred energy (Scheme 4a). Study of the fluorescence decay measurements of the terbium emission (at 545 nm) confirmed the existence of FRET in the NP-PS conjugate. $^1O_2$ generation by 44 kV X-ray excitation (5.4 mGy/s from a tungsten anode) was also observed using time-resolved laser spectroscopy and $^1O_2$ probes (singlet oxygen sensor green, SOSG and 3-*p*- (aminophenyl)fluorescein, APF) (Scheme 4b). Although the authors proposed to use this nanoscintillator construct for deep tissue PDT treatment combined with radiotherapy, animal experiments have not yet been demonstrated using this material.

Another gadolinium-based X-ray transducer NP has been reported as a liponanoparticle construct.[87] In this study, GdEuC12 micelles were integrated with hyperricin (Hyp) photosensitizer. GdEuC12 micelles alone had emission peaks at 595 and 618 nm, corresponding to Eu emission characteristics. The peak at 618 nm nicely overlapped the absorption peak of Hyp, implying that an efficient energy transfer from the lanthanide to PS could be achieved. Surprisingly, it was found that the micelle-PS system is localized in the nucleus, mostly in the nucleoli, of HeLa cells while the cells treated with hypericin alone showed fluorescence surrounding the nucleus. The idea of using micelles for this purpose has advantages, specifically in regard to drug loading, internalization, and nuclear localization. Nuclear localization was of particular interest because it was claimed that the cell nucleus is a more sensitive site for $^1O_2$ damage than other cell organelles.[88] In addition, some PSs might concentrate near the cell nucleus[89] and bind to nucleic acids.[90, 91] Proximity of PSs within 20 nm of the nucleus corresponds to an average intracellular diffusion distance of the $^1O_2$ produced during PDT, which results in enhanced toxicity to the tumor cells by induction of apoptosis or necrosis.[89, 92] This study demonstrates that efforts have been made to increase PS delivery to the cell nucleus due to the previously mentioned specific advantages.[93–96]

Another example of nuclear targeting was reported using nuclear targeted peptide (HIV-1 TAT) conjugated to a nanoscintillator.[97] Commercially available yttrium oxide (Y_2O_3) NPs were decorated with 2-chloroethylphosphonic acid (2-CEP) ligands that can form thioether linkages to the cell-penetrating and nuclear targeting HIV-1 TAT peptide (which bounds to psoralen). It was thought that Y_2O_3 nanoscintillators would absorb the X-ray photons then emit UVA light, which would induce the cross-linking of free psoralen to adenine and thymine residues in DNA (Figure 3). The crosslinking would then cause apoptosis *in vitro* and immunogenic response *in vivo*.[98–100] The results of the study showed a slight but

significant dose-dependent reduction trend in the growth of PC-3 prostate cancer cells with 2 Gy of 160 kVp or 320 kVp X-rays compared to cells containing psoralen-free Y_2O_3 nanoscintillators. Although using HIV-1 TAT peptides for targeting the nucleus is compelling, it would be even more useful if psoralen could continue the process without $^1O_2$ generation. A drug-peptide nanoconjugate with that particular characteristic would present itself as an ideal agent for treating deep-seated tumors in hypoxic environments.

Recently, lanthanide-doped nanoparticles, $SrAl_2O_4:Eu^{2+}$, were reported to convert X-ray photons to visible light that match the excitation wavelength of the merocyanine 540 (MC540) photosensitizer.[101] Remarkably, a single low X-ray dose (0.5 Gy) was sufficient to cause damage to the cancer cells both *in vitro* and *in vivo*. Moreover, this nanomaterial could reduce tumor growth rate in U87MG xenograft models without damaging the normal tissues. The $SrAl_2O_4:Eu^{2+}$ nanoscintillator was further found to be highly hydrolytic, and could be reduced to low-toxic ions and competently cleared from the body within two weeks.

The combination of a nanoscintillator and a semiconductor was introduced as a strategy for synchronous radiotherapy and ionizing-radiation-induced deep PDT with diminished oxygen dependence.[102] Ce^{3+}-doped $LiYF_4$ NPs (also considered ScNPs) were prepared as nanoconverters (X-rays to UV) after coating ZnO semiconductor NPs *via* metal-sulfur bonds (Figure 4a). Under X-ray irradiation, the SCNP core emitted low energy that matches the band gap of the semiconductor to generate hydroxyl radicals. The hydroxyl radical (•OH) dervied from the interaction between the hole (h^+) and water (not O_2 molecule) reduced the oxygen–tension dependency for the generation of the reactive oxygen species (Figure 4b). TEM images showed high uniformity and sharp particle size distribution with an average diameter of 33.8 nm of SZNP (Figure 4c–h). The chemical composition was further confirmed through a corresponding element mapping study (Figure 4i). The capability of this system was evaluated in live cells and *in vivo*. After exposing HeLa cells to X-rays (3 Gy), the normoxic (21% O_2) cells showed higher ROS generation than the hypoxic (2% O_2) cells. Furthermore, HeLa tumor bearing mice were treated with the nanoscintillator followed by X-ray irradiation (8 Gy). By Day 15 post-treatment, the tumor was almost completely eradicated after using this method, as seen in Figure 4j. However, there is still room for further optimization of the *in vivo* active tumor targeting efficacy of these fascinating nanoparticles.

Recently, cerium trifluoride (CeF_3) NPs were found to act as an efficient scintillator and were shown to emit visible light upon X- or γ-ray irradiation.[103] To demonstrate $^1O_2$ generation upon X-ray excitation, the NPs were conjugated with verteporfin (VP), a PS that predominantly undergoes the type II PDT mechanism. The SOSG was used as a probe to detect $^1O_2$ since it is highly specific for $^1O_2$ as compared to other ROS.[104] By using 8 keV X-ray irradiation, the $^1O_2$ quantum yield was determined to be 0.79 ± 0.05 for the conjugate with 31 molecules of VP per CeF_3 NP. In addition, the $^1O_2$ generation was estimated to be comparable to cytotoxic doses of O_2 per cell for PDT using light activation when a therapeutic dose of 60 Gy at 6 MeV (high energy) and 30 keV (low energy) was used. Although the cell viability was reported to be reduced when 6 MeV radiation energy was employed, the high energy X-rays were still needed, and most of the cells were found to be still alive (> 65 %). These results indicate that the energy transfer between NPs and the PS

was not very efficient, which might be due to the electrostatic interaction between NPs and the PS being unstable in the bioenvironment.

Metal-Based Nanoparticles

Similar to lanthanide-based, metal-based nanoscintillators were also introduced as X-ray transducers. In particular, strong X-ray excited luminescence has been observed in ZnO NPs,[75] and UV emission of the ZnO NPs matches well with the UV absorption of most porphyrins.[105] Therefore, the combination of ZnO and PS has been considered to be one of the best candidates for X-ray activated PDT. Chen and co-workers first reported *meso*-tetra(o-amino phenyl) porphyrin (MTAP) conjugated ZnO nanoparticles for PDT treatment of deep cancer.[106] In this study, the energy transfer efficiency from the ZnO NPs to MTAP was found to be as high as 83%. High phototoxicity in a human ovarian carcinoma cell line (NIH:OVCAR-3) was obtained using the ZnO-MTAP systems under UV illumination. Moreover, X-ray activated PDT using this combination is still under investigation.

Interestingly, zinc oxide (ZnO) was also reported as a potent radiosensitizer under X-ray irradiation without attaching it to a PS.[107] The synthesized ZnO/SiO_2 NPs in this study were found to be stable in water and culture media. The radiosensitizing ability of ZnO/SiO_2 was demonstrated in human prostate adenocarcinoma cell lines (LNCaP and Du145). Although ZnO NPs have been demonstrated to be a promising biocompatible material for biomedicinal applications, reports also showed the potential toxicity of ZnO harmonic NPs based on cellular assay studies.[108]

Chen and co-workers further reported using zinc-based nanoscintillators for X-ray activated PDT in a follow-up study.[109] In this work, tetrabromorhodamine-123 (TBrRh123) was conjugated to copper and cobalt co-doped ZnS (ZnS:Cu,Co). Results showed the combination had an efficient energy transfer and also displayed a long lasting afterglow, which could be a persistent light source for PDT even when the X-rays were turned off. Compared to the PS alone, this combination exhibited a high light-to-dark toxicity ratio in human prostate cancer cells (PC3).

The copper-cysteamine micro complex (Cu-Cy, size: 5–20 μm) is another type of scintillator material with intrinsic sensitizer characteristics that can produce $^1O_2$ under X-ray irradiation.[73] The rate of $^1O_2$ production from the Cu–Cy particles was higher than any other known photosensitizer using X-rays. Although the internalization of Cu-Cy particles in MCF-7 cells was found to be low, the materials could still efficiently cause significant damage to cancer cells when activated by X-ray irradiation (2 Gy). Furthermore, the Cu-Cy particles showed tumor destruction *in vivo* after intratumoral injection and exposure to a higher dose of X-rays (5 Gy). Although Cu-Cy could have a significant impact on deep tumor treatment, further optimization of surface modification, cellular uptake, and tumor active targeting efficacy is needed.

Non-Metal Based Radiosensitizers

SiC/SiO_x core/shell nanowires (NW) conjugated with tetra(*N*-propynyl-4-aminocarbonylphenyl)porphyrin (H_2TPACPP) *via* click chemistry were presented as a hybrid nanosystem for X-ray induced PDT.[111] Results showed that the NW-H_2TPACPP

nanosystem could generate $^1O_2$ efficiently enough to harm lung adenocarcinoma cells (A549 cells). Upon exposure to 6 MV of X-ray irradiation (2 Gy), the cell population was reduced by 75% after 12 days of treatment. Also, the increase in NW concentrations (100 and 500 mg/mL) together with a higher X-ray dose (6 Gy, single shot), demonstrated that the reduction of the intracellular amount of adenosine triphosphate (ATP) could also be achieved. The authors also claimed that an irradiation time of 20 seconds could be obtained from the experiment, which is significantly shorter than the standard clinical treatment times (40 s with single, 90 s with multiple irradiation fields). However, no evidence from *in vivo* studies was presented to support this assertion.

Previously, silicon NPs were investigated for their ability to increase ROS yield upon X-ray irradiation.[112] The results confirmed that cytotoxic $^1O_2$ was only generated in radiated solutions containing the NPs. The surface of the particles was oxidized to SiO_2, and the luminescence yield decreased with the irradiation dose. It was also found that changes in the surface morphology did not affect the yield of $^1O_2$ generation per Gy. It is known that glioma C6 cells are highly resistant to ionizing radiation. Nanoparticles taken by glioma C6 cells showed an enhanced cellular ROS production under X-ray exposure. However, no enhanced cellular ROS generation was observed in the absence of NPs upon X-ray irradiation.

Protoporphyrin IX (PpIX) is known as a potent drug for PDT. Although PpIX has been approved for use in the clinic, its low water solubility and skin accumulation provokes concerns about the side effects of radiation. Recently, Chen *et al.* modified PpIX by coating it with 3-aminopropyl triethoxysilane (APTES) to improve water solubility and stability.[110] The results indicated that the coating of APTES on PpIX principally increased its water dispersion, stability, and luminescence efficiency, which consequently increased the $^1O_2$ production efficacy. The authors were particularly interested in $^1O_2$ production directly induced by X-ray irradiation (without a nano-convertor). Interestingly, they found that $^1O_2$ could be detected in only the modified PpIX upon X-ray irradiation, implying its potential use in deep cancer treatment. However, the reported results of $^1O_2$ production in photosensitizers activated by X-rays are still controversial.[113–115]

Quantum Dots

Quantum dots (QDs) have also gained prevalence in their development as photosensitizers.[116, 117] The process of light-activated production of free radicals upon absorption of UV/visible light by a chromophore (such as QDs) can eradicate only surface-tumors due to the limitation of light penetration depth. Recently, QDs such as CdTe or CdSe/ZnS have been reported as X-ray or γ-ray scintillators for imaging applications.[118, 119] The interaction between QDs and X-rays is shown in Scheme 5.

Since X-rays and γ-rays can penetrate much deeper, their combination with QDs could serve as radiosensitizers to treat patients with deep tumors through PDT. Photocatalysts (*e.g.* TiO_2), scintillators (*e.g.* ZnS:Ag and CeF_3), and QDs (*e.g.* CdTe and CdSe) were chosen to analyze the potential of radiosensitizers induced by X-rays.[120] These materials contain heavy atoms that have large absorption coefficients combined with K-shell absorption edges in the spectrum range of a diagnostic X-ray generator. Generation of ROS under the

exposure of polychromatic X-rays was detected as a function of X-ray doses for all materials dispersed in aqueous solution, and the amount varied between the different the solution concentrations. For *in vitro* studies, HeLa cells were mixed with aqueous solutions dispersed with sensitizing materials (3.0 mg/mL) and exposed to different doses of X-rays. A survival assay was performed immediately after the irradiation. Unfortunately, the results showed only minor therapeutic effects at low X-ray doses. To improve the sensitization effect, bio-conjugated CdSe QDs were synthesized. The materials were internalized in the cytoplasm of HeLa cells up to a concentration of 1.0 ng/mL before being exposed to X-rays (up to 5 Gy). Results showed that the cell viability was reduced for the cells with QDs, implying that internalized QDs could serve as a more effective radiosensitizer.

X-rays with energy in the kilovoltage range are frequently used to activate ScNP-PS systems, whereas the megavoltage range beam is commonly used for conventional radiotherapy. There are not many reports on ScNPs that could be excited by higher X-ray doses and still improve the energy transfer efficiency for significant cell killing. To address these critical issues, amine-functionalized, Photofrin-conjugated PEGylated QDs were used as mediators to investigate the energy transfer from MV X-rays.[121] The linear relationship between a number of visible photons generated from QDs excited by 6-MV X-rays and the radiation dose rate was observed. The energy transfer process efficiency reached 100% once the number of conjugated-Photofrin molecules increased. A significant H460 human lung carcinoma cell killing efficacy was perceived from the combined radiation and PDT treatment when compared to radiation alone. These results could be highly useful for clinical applications in the prediction of light dosimetry.

Radionuclide-Activated Photodynamic Therapy

Cerenkov Radiation Activating Phototherapy

The use of photons from Cerenkov radiation (CR) has been emerging for optical imaging and activating QDs and fluorophores *in vivo*.[122–126] Charged particles, such as β^+ and β^-, generated from radioactive decay can emit visible light in a broad energy range while moving through a dielectric medium at a speed greater than the velocity of light. CR can be used to directly activate the fluorophore/phosphor without any requirements regarding the NPs.

As a proof-of-concept, CR was reported as an internal light source to activate cage compounds *in vivo*.[126] 2-deoxy-2-[^{18}F]fluoro-D-glucose (^{18}FDG), a positron emission tomography (PET) radiotracer, was used as an activating light for uncage luciferin 1-(4,5-dimethoxy-2-nitrophenyl) ethyl ester (DMNP-luciferin) in a breast cancer animal model expressing luciferase (MDA-MB-231-luc-D3H1). Real-time monitoring of the luciferin bioluminescence produced was observed under CR-activated uncaging of substrate (as shown in Figure 5).

In traditional PDT, light is given to photosensitive materials to generate $^1O_2$ that are toxic to induce cell death. However, the technique only works well when light and oxygen can localize in the treatment site. Recently, Schilefu *et. al.* conceived a way to deliver light directly to the tumor instead of applying light from an outside source.[76] CR induced by beta

particles was used as a light source to activate NPs that act as oxygen-independent photosensitizers. After looking at a number of options, the researchers focused on NPs made of titanium dioxide (TiO_2), and used ^{18}FDG as an activation source. When exposed to light, TiO_2 NPs produce free radicals without requiring oxygen. It was hypothesized that the radioactive fluorine would produce enough CR to activate a photosensitizing agent if it could also be delivered to the same location. In this way, ^{18}FDG could serve two purposes. First, it would continue its role as a PET imaging isotope; second, it would acquire the function of providing light for phototherapy. To increase the therapeutic efficiency, the investigators also added a drug called titanocene (Tc, an initially approved drug that failed in phase II clinical trials due to an undesirable effect) to the TiO_2 surface. The NPs were further coated with transferrin (Tf) to form TiO_2-Tf-Tc for specific tumor accumulation. Different formulations of the NPs and cancer drug combined with the ^{18}FDG light source were tested in mice with human lung tumors (A549) and fibrosarcoma tumors (HT1080), or tumors of the connective tissue. The following combinations were used to test the therapeutic effects: ^{18}FDG plus the tumor-seeking nanoparticles alone (TiO_2-Tf), ^{18}FDG plus the tumor-seeking cancer drug alone (Tc-Tf), and ^{18}FDG plus the tumor-seeking nanoparticles carrying the cancer drug (TiO_2-Tf-Tc). When a single dose (1 mg/kg) was injected into the bloodstream with ^{18}FDG, TiO_2-Tf-Tc was found to have the most significant treatment effect. Fifteen days after treatment, tumors in the treated mice were eight times smaller than those in untreated mice, and survival increased to 50 days, compared with 30 days for both TiO_2-Tf and Tf-Tc NP groups (Figure 6). Histological analysis did not reveal significant toxicity in the liver and kidneys after treatment, indicating the absence of systemic toxicity. Overall, this inventive approach opens up the possibility of treating a variety of lesions in a depth- and oxygen-independent manner.

Based on the idea given above, CR could be more powerful if higher energy β emitters are employed, such as yttrium-90 (2,280 keV) or zirconium-89 (909 keV), rather than using either fluorene-18 (633 keV) or copper-64 (574 keV). Additionally, modification of the NP surface could be achieved to increase tumor selectivity, while a combination of NPs and PSs could be used to enhance therapeutic efficacy.

Nanoparticle-Mediated Radioisotope Energy Transfer

Cerenkov luminescence imaging (CLI) offers significant possibilities in clinical translation because many tracers which produce Cerenkov light have already been approved for clinical use. However, CLI is still restricted by its limitations. When compared with conventional fluorescence imaging, Cerenkov luminescence intensity is several orders of magnitude weaker since most of the radiated energy is in γ photons or other emitted particles. Moreover, CR is mainly composed of UV-blue photons, which limit its tissue penetration depth. One promising strategy to improve CLI involves using energy transfer mediators (such as QDs[127, 128] or gold nanoparticles[129]), which convert CR to a longer wavelength in order to detect deep-seated tumors. This technique is known as Cerenkov radiation energy transfer (CRET). Unfortunately, the energy transfer efficiency might be an issue with this technique and could potentially limit imaging sensitivity *in vivo*.

To enhance the optical signal and improve the energy activation process, europium oxide (EO) nanoparticles were introduced to convert γ-radiation (a major decay particle) and Cerenkov luminescence (CL, a minor decay particle) into fluorescence.[130] To evaluate this concept, three radioactive tracers were used, ^{18}F-FDG, ^{99m}Tc-MDP (methylene diphosphonate) and ^{131}I-NaI. ^{18}FDG emits γ-radiation (511 keV), β^+ particles and CL, ^{99m}Tc-MDP only emits γ-ray (140 keV), and ^{131}I-NaI emits major γ-ray (364 keV). It was found that EO nanoparticles can be excited in the UV-blue range to generate red emission peaking at 620 nm, indicating CL was capable of activating EO. Placing radiotracers in a separate container with EO could also activate the NPs; however, the luminescence intensity depended on the excitation distance. By using different types of radiotracers, it was found that γ-ray was the major excitation source. Although, mixing radiotracers with EO gave different results, which the authors attributed to Compton scattering and the photoelectric effect of γ photons from the optical signals. For further validation of the superior radiotracer-excited fluorescence imaging, the NPs were tested in Bcap-37 (human breast cancer cells) and U87MG (human glioblastoma cells) xenografts in mice. After direct intratumoral injection with EO (0.05 mg) into the Bcap-37 xenografts and tail-vein injection of ^{18}FDG (800 μCi), γ-ray activated fluorescence provided the best tumor to normal tissue contrast, as compared to Cerenkov luminescence and standard fluorescence imaging modalities. After tail-vein injection with EO (0.1 mg, 24 h prior) and ^{18}FDG (500 μCi) in the U87MG-xenografted mice, γ-ray activated fluorescence displayed significantly greater signal than CLI with both no filtering and 620-nm filtering, illustrating the passive targeting of the NPs in the tumor tissue. Moreover, no obvious toxicity was observed after four weeks of experiments.

Recently, other lanthanide-based radioluminescent microparticles were also developed as a proof-of-concept study that the materials can be activated by γ-rays emitted from radionuclides rather than CR.[131] Terbium doped Gd_2O_2S (Gd_2O_2S:Tb) nanomaterials were reported as X-ray nanophosphors and synthesized using complex precipitation methods.[132] In this study, Gd_2O_2S:Tb was activated by ^{18}FDG, resulting in the enhancement of luminescence excited by γ-rays. Although the potential use of this material in luminescence imaging has been well established, the biocompatibility of Gd_2O_2S:Tb might be a significant concern for future clinical translation. Other limitations include the short emission wavelength (520–550 nm) and the unidentified tumor-targeting efficacy.

Overall, this internal light activation strategy offers high sensitivity imaging and supports the claim that γ-rays might be a better source for fluorophore excitation than current methods. The technique can also be applied to PDT, since γ-radiation can be an internal light source to activate photosensitizers to generate $^1O_2$ for cancer treatment (Scheme 6).

Conclusions and Future Perspectives

PDT offers high selectivity and marginal invasion in cancer treatment. However, the light penetration depth of traditional PDT is still limited. Nanotechnology plays a significant role in developing strategies to treat deep-seated cancer using PDT. The past five years have witnessed rapid growth in using X-rays as the light source for treating deep-seated tumors pre-clinically. Due to the fact that PSs cannot absorb X-rays, ScNPs have been developed as

both the nanocarriers and energy transducers for X-ray induced PDT. Rare-earth element based NPs have gained increasing attention in X-ray excited PDT because of their tunable emission wavelengths. Various PSs, *e.g.* organic dyes and QDs, are options for developing effective PDT agents. Table 1 Summarizes ScNPs that used as X-ray mediators for PDT purposes. A similar summary of NPs for deep-seated PDT using other approaches can be found elsewhere.[12, 13] Once X-rays began to emerge as a powerful external light source for PDT, radioisotopes were also explored as an internal activation source for PDT. This can be beneficial since no exterior light is required, and higher energy and longer half-life radioisotopes would trigger the PDT process more efficiently.

Although tissue penetration depth is not a problem for either modalities (X-ray and radioisotope-activated PDT), there is still room for improving the energy transfer efficiency and $^1O_2$ generation rate. Currently, the existing nanosystems for X-ray excited PDT are still not as effective as NIR-excited PDT. This is because the energy transfer from the ScNPs to the PS is quite critical and requires an excellent overlap between the emission peaks of the NPs and the absorption peaks of the PS. Therefore, the development of better nanocomposites for more efficient excitation/photosensitization is necessary.

To achieve this, X-ray ScNPs with a suitable size and strong luminescence are necessary. In general, higher atomic number phosphors have greater radiation stopping power and a higher absorption coefficient for radiation, resulting in a strong luminescence emission.[133, 134] NPs with small diameters are preferable as they have a weak electron–phonon coupling and subsequently exhibit greater luminescence efficiency due to a smaller Stokes shift.[135] Moreover, the distance (<10 nm) between the donor and the acceptor is crucial for efficient energy transfer. In addition, the PS should also have high $^1O_2$ quantum yield and photostability.

Biocompatibility and long-term toxicity of nanocomposites need to be well-studied. Plausible toxicity of NPs is mainly from two mechanisms: (i) NPs can enter the body through the skin, lungs, or intestinal tract, deposit in several organs, and may cause adverse biological reactions, and (ii) toxicity can come from components in the material, such as CdSe/CdTe in QDs or rare earth elements (especially Ce, La and Gd) in NPs. [136, 137] Recently, nanotoxicology has appeared as a branch of toxicology for studying the undesirable effects of nanoparticles.[138, 139] Since X-ray excited PDT is expected to be applicable in the clinic, delivering PSs systematically to tumor sites is essential. For this purpose, NPs need to be stable enough to deliver the PS to the tumor and gradually degrade away after therapy. In this case, biodegradable nanomaterials could be a good option to minimize potential toxicity. Systematic safety evaluations of nanomaterials must also be taken into serious consideration alongside the optimization of X-ray doses.

In vivo systematic tumor targeting efficacy is still one of the major challenges for nanoparticles. Although X-ray beams can be focused on the tumor area, it is still difficult to control for the deep-seated tumors. Most NPs target tumors *via* the EPR effect by taking advantage of the leaky tumor environment and the long-circulation of NPs in the blood stream. Although this can be therapeutically useful in some cases, it also causes prolonged normal tissue exposure to the PS, which can give rise to undesirable toxicity. One possibility

to improve tumor targeting efficacy is by targeting tumor vasculature instead of tumor cells since many NPs are too large to be extravasated.[21, 140–144] Additionally, the compact size and optimized surface features of the NPs are desirable to minimize the uptake by the reticuloendothelial system (RES) and maximize the tumor accumulation rate.[143, 145]

Most nanocomposites reported so far for X-ray excited PDT only showed the tumor treatment *via* intratumoral injection on subcutaneous tumor models. It is relatively easy to produce the tumor models, and intratumoral injection is to ensure that all materials are located at the tumor site. Before clinical translation is possible, studies on orthotopic tumor models are crucial. To achieve this, the nanocomposites must be well-modified and be stable enough for intravenous (iv.) injection, as well as be able to target the tumor at the actual site.

To enhance therapy efficiency, X-ray activated PSs *via* nanoscintillators can be combined with radiotherapy to treat diseases that are endoscopically inaccessible. Some nanoconstructs that have previously been combined in this manner are synchronous radio- and PDT,[102] or chemo-/radio-/PDT.[146] Moreover, the materials that possess high efficiency X-ray scintillation[60, 63] could be good candidates for energy transducers.

Presently, radiotherapy has evolved beyond the capabilities of X-ray technology for these applications. Many external beam radiation treatment (EBRT) methods exist today that allow for higher precision and conformity in the delivered dose distributions. Among these, intensity-modulated radiation therapy (IMRT) and Tomotherapy hold promise to work in conjunction with X-ray excited PDT. By using an excitation technique with higher dose conformity, the therapeutic index of the combined PDT/EBRT may be maximized. The basic premise of IMRT is to modify the intensity of the incoming radiation beam during the treatment. The radiotherapy dose is then altered depending on the thickness of the body tissue. In this case, cancer gets the same dose across the treatment area. It also allows the radiotherapy beam to be shaped more accurately and directed at the cancer while avoiding the surrounding normal tissue. This can be done by blocking the normal tissues using the multileaf collimators (MLCs) of the beam and using multiple linac gantry angles to achieve the desired dose distribution.[147] IMRT may be performed with the traditional linac energies (6MV and 10MV). Similarly, Tomotherapy provides a more conformal dose distribution. In the same way as IMRT, the intensity of the beam is modulated during this treatment as well. However, in this case, the patient moves through the bore of the linac during the treatment, essentially being treated in “slices”.[148] Tomotherapy also carries the capability for on-board imaging (using a megavoltage CT scanner) which can help in tumor localization. The nominal energies of the beam in Tomotherapy are 6 MV for the treatment, and 3.5 MV for the imaging capabilities.[149]

Overall, nanotechnology has provided excellent opportunities for the treatment of deep-seated tumors. X-ray excited PDT is a great concept in oncological treatment, especially since many efforts have been devoted to developing nanomaterials for this therapy. However, there are still challenges to overcome, including finding the best one(s) for clinical translation. This challenge was addressed in this review, as strategies to improve ScNP-PS are suggested. Further discussion and collaboration among scientists, clinicians, engineers, and pharmacists could aid PDT in being an effective treatment modality in oncology.

Moreover, the newly funded Centers of Cancer Nanotechnology Excellence (CCNEs) may play important roles in the future of nanooncology by leading the field and painting the future.

Acknowledgments

This work is supported, in part, by the University of Wisconsin - Madison, the National Institutes of Health (NIBIB/NCI 1R01CA169365, P30CA014520, and T32GM008349), and the American Cancer Society (125246-RSG-13-099-01-CCE). The National Basic Research and Development Program of China (973) under Grant No. 2011CB707702 and the National Natural Science Foundation of China under Grant No. 81101100.

VOCABULARY

Scintillator	a substance that glows when hit by high-energy particles or photons
Photosensitizer	a compound that can react with light to cause a sensitivity reaction in the substance or organism
Photodynamic therapy	a form of phototherapy using nontoxic light-sensitive compounds that becomes toxic to targeted cells when they are exposed to a certain wavelength of light
Radiation therapy	a therapy using ionizing radiation to control or kill cells
Ionizing radiation	radiation that carries enough energy to release electrons from atoms or molecules. Gamma rays, X-rays and the higher ultraviolet part of the electromagnetic spectrum are considered ionizing radiation
Phosphor	a substance that exhibits luminescence when excited by radiation

References

1. Agostinis P, Berg K, Cengel KA, Foster TH, Girotti AW, Gollnick SO, Hahn SM, Hamblin MR, Juzeniene A, Kessel D, Korbelik M, Moan J, Mroz P, Nowis D, Piette J, Wilson BC, Golab J. Photodynamic Therapy of Cancer: An Update. CA Cancer J Clin. 2011; 61:250–281. [PubMed: 21617154]
2. Dougherty TJ, Gomer CJ, Henderson BW, Jori G, Kessel D, Korbelik M, Moan J, Peng Q. Photodynamic Therapy. J Natl Cancer Inst. 1998; 90:889–905. [PubMed: 9637138]
3. DeRosa MC, Crutchley RJ. Photosensitized Singlet Oxygen and Its Applications. Coord Chem Rev. 2002; 233:351–371.
4. Jacques SL. Optical Properties of Biological Tissues: A Review. Phys Med Biol. 2013; 58:R37–61. [PubMed: 23666068]
5. Ethirajan M, Chen Y, Joshi P, Pandey RK. The Role of Porphyrin Chemistry in Tumor Imaging and Photodynamic Therapy. Chem Soc Rev. 2011; 40:340–362. [PubMed: 20694259]
6. Smith AM, Mancini MC, Nie S. Bioimaging: Second Window for *in Vivo* Imaging. Nat Nanotechnol. 2009; 4:710–711. [PubMed: 19898521]
7. Rosenthal I. Phthalocyanines as Photodynamic Sensitizers. Photochem Photobiol. 1991; 53:859–870. [PubMed: 1886943]
8. Luo S, Zhang E, Su Y, Cheng T, Shi C. A Review of NIR Dyes in Cancer Targeting and Imaging. Biomaterials. 2011; 32:7127–7138. [PubMed: 21724249]

9. Wilson BC. Photodynamic Therapy for Cancer: Principles. Can J Gastroenterol. 2002; 16:393–396. [PubMed: 12096303]
10. Zwijnenburg MA. Photoluminescence in Semiconductor Nanoparticles: An Atomistic View of Excited State Relaxation in Nanosized Zns. Nanoscale. 2012; 4:3711–3717. [PubMed: 22595975]
11. Al-Sayyed G, D'Oliveira JC, Pichat P. Semiconductor-Sensitized Photodegradation of 4-Chlorophenol in Water. J Photochem Photobiol A. 1991; 58:99–114.
12. Lucky SS, Soo KC, Zhang Y. Nanoparticles in Photodynamic Therapy. Chem Rev. 2015; 115:1990–2042. [PubMed: 25602130]
13. Hu J, Tang Y, Elmenoufy AH, Xu H, Cheng Z, Yang X. Nanocomposite-Based Photodynamic Therapy Strategies for Deep Tumor Treatment. Small. 2015; 11:5860–5887. [PubMed: 26398119]
14. Idris NM, Gnanasammandhan MK, Zhang J, Ho PC, Mahendran R, Zhang Y. *In Vivo* Photodynamic Therapy Using Upconversion Nanoparticles as Remote-Controlled Nanotransducers. Nat Med. 2012; 18:1580–1585. [PubMed: 22983397]
15. Wang C, Cheng L, Liu Z. Upconversion Nanoparticles for Photodynamic Therapy and Other Cancer Therapeutics. Theranostics. 2013; 3:317–330. [PubMed: 23650479]
16. Punjabi A, Wu X, Tokatli-Apollon A, El-Rifai M, Lee H, Zhang Y, Wang C, Liu Z, Chan EM, Duan C, Han G. Amplifying the Red-Emission of Upconverting Nanoparticles for Biocompatible Clinically Used Prodrug-Induced Photodynamic Therapy. ACS Nano. 2014; 8:10621–10630. [PubMed: 25291544]
17. Chen F, Zhang S, Bu W, Chen Y, Xiao Q, Liu J, Xing H, Zhou L, Peng W, Shi J. A Uniform Sub-50 nm-Sized Magnetic/Upconversion Fluorescent Bimodal Imaging Agent Capable of Generating Singlet Oxygen by Using a 980 nm Laser. Chemistry. 2012; 18:7082–7090. [PubMed: 22544381]
18. Bertrand N, Wu J, Xu X, Kamaly N, Farokhzad OC. Cancer Nanotechnology: The Impact of Passive and Active Targeting in the Era of Modern Cancer Biology. Adv Drug Deliv Rev. 2014; 66:2–25. [PubMed: 24270007]
19. Wang AZ, Langer R, Farokhzad OC. Nanoparticle Delivery of Cancer Drugs. Annu Rev Med. 2012; 63:185–198. [PubMed: 21888516]
20. Hong H, Wang F, Zhang Y, Graves SA, Eddine SB, Yang Y, Theuer CP, Nickles RJ, Wang X, Cai W. Red Fluorescent Zinc Oxide Nanoparticle: A Novel Platform for Cancer Targeting. ACS Appl Mater Interfaces. 2015; 7:3373–3381. [PubMed: 25607242]
21. Hong H, Yang K, Zhang Y, Engle JW, Feng L, Yang Y, Nayak TR, Goel S, Bean J, Theuer CP, Barnhart TE, Liu Z, Cai W. *In Vivo* Targeting and Imaging of Tumor Vasculature with Radiolabeled, Antibody-Conjugated Nanographene. ACS Nano. 2012; 6:2361–2370. [PubMed: 22339280]
22. Chen F, Hong H, Zhang Y, Valdovinos HF, Shi S, Kwon GS, Theuer CP, Barnhart TE, Cai W. *In Vivo* Tumor Targeting and Image-Guided Drug Delivery with Antibody-Conjugated, Radiolabeled Mesoporous Silica Nanoparticles. ACS Nano. 2013; 7:9027–9039. [PubMed: 24083623]
23. Chen F, Nayak TR, Goel S, Valdovinos HF, Hong H, Theuer CP, Barnhart TE, Cai W. *In Vivo* Tumor Vasculature Targeted PET/NIRF Imaging with TRC105(Fab)-Conjugated, Dual-Labeled Mesoporous Silica Nanoparticles. Mol Pharmaceutics. 2014; 11:4007–4014.
24. Byrne JD, Betancourt T, Brannon-Peppas L. Active Targeting Schemes for Nanoparticle Systems in Cancer Therapeutics. Adv Drug Deliv Rev. 2008; 60:1615–1626. [PubMed: 18840489]
25. Bazak R, Houri M, El Achy S, Kamel S, Refaat T. Cancer Active Targeting by Nanoparticles: A Comprehensive Review of Literature. J Cancer Res Clin Oncol. 2015; 141:769–784. [PubMed: 25005786]
26. Gu Z, Yan L, Tian G, Li S, Chai Z, Zhao Y. Recent Advances in Design and Fabrication of Upconversion Nanoparticles and Their Safe Theranostic Applications. Adv Mater. 2013; 25:3758–3779. [PubMed: 23813588]
27. Lim CK, Heo J, Shin S, Jeong K, Seo YH, Jang WD, Park CR, Park SY, Kim S, Kwon IC. Nanophotosensitizers toward Advanced Photodynamic Therapy of Cancer. Cancer Lett. 2013; 334:176–187. [PubMed: 23017942]

28. Tian G, Gu Z, Zhou L, Yin W, Liu X, Yan L, Jin S, Ren W, Xing G, Li S, Zhao Y. Mn2+ Dopant-Controlled Synthesis of NaYF4:Yb/Er Upconversion Nanoparticles for *in Vivo* Imaging and Drug Delivery. Adv Mater. 2012; 24:1226–1231. [PubMed: 22282270]
29. Chen W, Zhang J. Using Nanoparticles to Enable Simultaneous Radiation and Photodynamic Therapies for Cancer Treatment. J Nanosci Nanotechnol. 2006; 6:1159–1166. [PubMed: 16736782]
30. Blasse G. Scintillator Materials. Chem Mater. 1994; 6:1465–1475.
31. Nikl M. Scintillation Detectors for X-Rays. Meas Sci Technol. 2006; 17:R37–R54.
32. Seco J, Clasie B, Partridge M. Review on the Characteristics of Radiation Detectors for Dosimetry and Imaging. Phys Med Biol. 2014; 59:R303–347. [PubMed: 25229250]
33. Hill R, Healy B, Holloway L, Kuncic Z, Thwaites D, Baldock C. Advances in Kilovoltage X-Ray Beam Dosimetry. Phys Med Biol. 2014; 59:R183–231. [PubMed: 24584183]
34. Kobayashi K, Usami N, Porcel E, Lacombe S, Le Sech C. Enhancement of Radiation Effect by Heavy Elements. Mutat Res. 2010; 704:123–131. [PubMed: 20074660]
35. Boeckman HJ, Trego KS, Turchi JJ. Cisplatin Sensitizes Cancer Cells to Ionizing Radiation *via* Inhibition of Nonhomologous End Joining. Mol Cancer Res. 2005; 3:277–285. [PubMed: 15886299]
36. Band IM, Kharitonov YI, Trzhaskovskaya MB. Photoionization Cross Sections and Photoelectron Angular Distributions for X-Ray Line Energies in the Range 0.132–4.509 Kev Targets: $1 \leq Z \leq 100$. At Data Nucl Data Tables. 1979; 23:443–505.
37. Allisy-Roberts, P.; Williams, JR. Farr's Physics for Medical Imaging. Saunders; 2007.
38. Fernandez-Suarez M, Ting AY. Fluorescent Probes for Super-Resolution Imaging in Living Cells. Nat Rev Mol Cell Biol. 2008; 9:929–943. [PubMed: 19002208]
39. Sakdinawat A, Attwood D. Nanoscale X-Ray Imaging. Nat Photonics. 2010; 4:840–848.
40. Chao W, Harteneck BD, Liddle JA, Anderson EH, Attwood DT. Soft X-Ray Microscopy at a Spatial Resolution Better Than 15 nm. Nature. 2005; 435:1210–1213. [PubMed: 15988520]
41. Mimura H, Handa S, Kimura T, Yumoto H, Yamakawa D, Yokoyama H, Matsuyama S, Inagaki K, Yamamura K, Sano Y, Tamasaku K, Nishino Y, Yabashi M, Ishikawa T, Yamauchi K. Breaking the 10 nm Barrier in Hard-X-Ray Focusing. Nat Phys. 2010; 6:122–125.
42. Huda W, Abrahams RB. X-Ray-Based Medical Imaging and Resolution. AJR Am J Roentgenol. 2015; 204:W393–397. [PubMed: 25794088]
43. Leong AF, Fouras A, Islam MS, Wallace MJ, Hooper SB, Kitchen MJ. High Spatiotemporal Resolution Measurement of Regional Lung Air Volumes from 2D Phase Contrast X-Ray Images. Med Phys. 2013; 40:041909. [PubMed: 23556903]
44. Paunesku T, Vogt S, Maser J, Lai B, Woloschak G. X-Ray Fluorescence Microprobe Imaging in Biology and Medicine. J Cell Biochem. 2006; 99:1489–1502. [PubMed: 17006954]
45. Zhou SA, Brahme A. Development of Phase-Contrast X-Ray Imaging Techniques and Potential Medical Applications. Phys Med. 2008; 24:129–148. [PubMed: 18602852]
46. Lusic H, Grinstaff MW. X-Ray-Computed Tomography Contrast Agents. Chem Rev. 2013; 113:1641–1666. [PubMed: 23210836]
47. Chen H, Rogalski MM, Anker JN. Advances in Functional X-Ray Imaging Techniques and Contrast Agents. Phys Chem Chem Phys. 2012; 14:13469–13486. [PubMed: 22962667]
48. Ahmad M, Pratx G, Bazalova M, Lei X. X-Ray Luminescence and X-Ray Fluorescence Computed Tomography: New Molecular Imaging Modalities. IEEE Access. 2014; 2:1051–1061.
49. Pratx G, Carpenter CM, Sun C, Rao RP, Xing L. Tomographic Molecular Imaging of X-Ray-Excitable Nanoparticles. Opt Lett. 2010; 35:3345–3347. [PubMed: 20967061]
50. van Eijk CW. Inorganic Scintillators in Medical Imaging. Phys Med Biol. 2002; 47:R85–106. [PubMed: 12030568]
51. Feldmann C, Justel T, Ronda CR, Schmidt PJ. Inorganic Luminescent Materials: 100 Years of Research and Application. Adv Funct Mater. 2003; 13:511–516.
52. Zhu Y, Earnest T, Huang Q, Cai X, Wang Z, Wu Z, Fan C. Synchrotron-Based X-Ray-Sensitive Nanoprobes for Cellular Imaging. Adv Mater. 2014; 26:7889–7895. [PubMed: 24687860]

53. Wu C, Chiu DT. Highly Fluorescent Semiconducting Polymer Dots for Biology and Medicine. Angew Chem Int Ed Engl. 2013; 52:3086–3109. [PubMed: 23307291]
54. Campbell IH, Crone BK. Efficient Plastic Scintillators Utilizing Phosphorescent Dopants. Appl Phys Lett. 2007; 90:012117.
55. Osakada Y, Pratx G, Hanson L, Solomon PE, Xing L, Cui B. X-Ray Excitable Luminescent Polymer Dots Doped with an Iridium(III) Complex. Chem Commun. 2013; 49:4319–4321.
56. Wojtowicz AJ. Rare-Earth-Activated Wide Bandgap Materials for Scintillators. Nucl Instrum Methods Phys Res Sect A. 2002; 486:201–207.
57. Shi SK, Hossu M, Hall R, Chen W. Solution Combustion Synthesis, Photoluminescence and X-Ray Luminescence of Eu-Doped Nanoceria CeO_2:Eu. J Mater Chem. 2012; 22:23461–23467.
58. Yermolayeva YV, Korshikova TI, Tolmachev AV, Yavetskiy RP. X-Ray Luminescence of Core-Shell Structured SiO_2/Lu_2O_3:Eu3+ and $SiO_2/Lu_2Si_2O_7$:Eu3+ Particles. Radiat Meas. 2011; 46:551–554.
59. Osakada Y, Pratx G, Sun C, Sakamoto M, Ahmad M, Volotskova O, Ong Q, Teranishi T, Harada Y, Xing L, Cui B. Hard X-Ray-Induced Optical Luminescence *via* Biomolecule-Directed Metal Clusters. Chem Commun. 2014; 50:3549–3551.
60. Sudheendra L, Das GK, Li C, Stark D, Cena J, Cherry S, Kennedy IM. NaGdF:Eu Nanoparticles for Enhanced X-Ray Excited Optical Imaging. Chem Mater. 2014; 26:1881–1888. [PubMed: 24803724]
61. Sudheendra L, Ortalan V, Dey S, Browning ND, Kennedy IM. Plasmonic Enhanced Emissions from Cubic NaYF(4):Yb: Er/Tm Nanophosphors. Chem Mater. 2011; 23:2987–2993. [PubMed: 21709812]
62. Chen H, Moore T, Qi B, Colvin DC, Jelen EK, Hitchcock DA, He J, Mefford OT, Gore JC, Alexis F, Anker JN. Monitoring pH-Triggered Drug Release from Radioluminescent Nanocapsules with X-Ray Excited Optical Luminescence. ACS Nano. 2013; 7:1178–1187. [PubMed: 23281651]
63. Wang C, Volotskova O, Lu K, Ahmad M, Sun C, Xing L, Lin W. Synergistic Assembly of Heavy Metal Clusters and Luminescent Organic Bridging Ligands in Metal-Organic Frameworks for Highly Efficient X-Ray Scintillation. J Am Chem Soc. 2014; 136:6171–6174. [PubMed: 24730683]
64. Sun C, Pratx G, Carpenter CM, Liu H, Cheng Z, Gambhir SS, Xing L. Synthesis and Radioluminescence of Pegylated Eu(3+) -Doped Nanophosphors as Bioimaging Probes. Adv Mater. 2011; 23:H195–199. [PubMed: 21557339]
65. Naczynski DJ, Sun C, Turkcan S, Jenkins C, Koh AL, Ikeda D, Pratx G, Xing L. X-Ray-Induced Shortwave Infrared Biomedical Imaging Using Rare-Earth Nanoprobes. Nano Lett. 2015; 15:96–102. [PubMed: 25485705]
66. Dolmans DE, Fukumura D, Jain RK. Photodynamic Therapy for Cancer. Nat Rev Cancer. 2003; 3:380–387. [PubMed: 12724736]
67. Moan J, Berg K. The Photodegradation of Porphyrins in Cells Can Be Used to Estimate the Lifetime of Singlet Oxygen. Photochem Photobiol. 1991; 53:549–553. [PubMed: 1830395]
68. Allison RR, Downie GH, Cuenca R, Hu XH, Childs CJ, Sibata CH. Photosensitizers in Clinical PDT. Photodiagn Photodyn Ther. 2004; 1:27–42.
69. Li LB, Luo RC, Liao WJ, Zhang MJ, Luo YL, Miao JX. Clinical Study of Photofrin Photodynamic Therapy for the Treatment of Relapse Nasopharyngeal Carcinoma. Photodiagn Photodyn Ther. 2006; 3:266–271.
70. Yang P, Gai S, Lin J. Functionalized Mesoporous Silica Materials for Controlled Drug Delivery. Chem Soc Rev. 2012; 41:3679–3698. [PubMed: 22441299]
71. Yuan Q, Wu Y, Wang J, Lu D, Zhao Z, Liu T, Zhang X, Tan W. Targeted Bioimaging and Photodynamic Therapy Nanoplatform Using an Aptamer-Guided G-Quadruplex DNA Carrier and near-Infrared Light. Angew Chem Int Ed Engl. 2013; 52:13965–13969. [PubMed: 24281972]
72. Yu Z, Sun Q, Pan W, Li N, Tang B. A Near-Infrared Triggered Nanophotosensitizer Inducing Domino Effect on Mitochondrial Reactive Oxygen Species Burst for Cancer Therapy. ACS Nano. 2015; 9:11064–11074. [PubMed: 26456218]
73. Zou X, Yao M, Ma L, Hossu M, Han X, Juzenas P, Chen W. X-Ray-Induced Nanoparticle-Based Photodynamic Therapy of Cancer. Nanomedicine (London, U K). 2014; 9:2339–2351.

74. Kuznetsova NA, Gretsova NS, Derkacheva VM, Kaliya OL, Lukyanets EA. Sulfonated Phthalocyanines: Aggregation and Singlet Oxygen Quantum Yield in Aqueous Solutions. J Porphyrins Phthalocyanines. 2003; 7:147–154.
75. Armelao L, Heigl F, Jurgensen A, Blyth RIR, Regier T, Zhou XT, Sham TK. X-Ray Excited Optical Luminescence Studies of ZnO and Eu-Doped ZnO Nanostructures. J Phys Chem C. 2007; 111:10194–10200.
76. Kotagiri N, Sudlow GP, Akers WJ, Achilefu S. Breaking the Depth Dependency of Phototherapy with Cerenkov Radiation and Low-Radiance-Responsive Nanophotosensitizers. Nat Nanotechnol. 2015; 10:370–379. [PubMed: 25751304]
77. Hou Z, Zhang Y, Deng K, Chen Y, Li X, Deng X, Cheng Z, Lian H, Li C, Lin J. Uv-Emitting Upconversion-Based TiO_2 Photosensitizing Nanoplatform: Near-Infrared Light Mediated *in Vivo* Photodynamic Therapy *via* Mitochondria-Involved Apoptosis Pathway. ACS Nano. 2015; 9:2584–2599. [PubMed: 25692960]
78. Zeng L, Pan Y, Tian Y, Wang X, Ren W, Wang S, Lu G, Wu A. Doxorubicin-Loaded NaYF4:Yb/Tm-TiO_2 Inorganic Photosensitizers for NIR-Triggered Photodynamic Therapy and Enhanced Chemotherapy in Drug-Resistant Breast Cancers. Biomaterials. 2015; 57:93–106. [PubMed: 25913254]
79. Chen W. Nanoparticle Self-Lighting Photodynamic Therapy for Cancer Treatment. J Biomed Nanotechnol. 2008; 4:369–376.
80. Liu YF, Chen W, Wang SP, Joly AG. Investigation of Water-Soluble X-Ray Luminescence Nanoparticles for Photodynamic Activation. Appl Phys Lett. 2008; 92:043901.
81. Khan, FM. The Physics of Radiation Therapy. Lippincott Williams & Wilkins; 2003.
82. Tang Y, Hu J, Elmenoufy AH, Yang X. Highly Efficient Fret System Capable of Deep Photodynamic Therapy Established on X-Ray Excited Mesoporous LaF3:Tb Scintillating Nanoparticles. ACS Appl Mater Interfaces. 2015; 7:12261–12269. [PubMed: 25974980]
83. Elmenoufy AH, Tang Y, Hu J, Xu H, Yang X. A Novel Deep Photodynamic Therapy Modality Combined with CT Imaging Established *via* X-Ray Stimulated Silica-Modified Lanthanide Scintillating Nanoparticles. Chem Commun. 2015; 51:12247–12250.
84. Abliz E, Collins JE, Bell H, Tata DB. Novel Applications of Diagnostic X-Rays in Activating a Clinical Photodynamic Drug: Photofrin II through X-Ray Induced Visible Luminescence from “Rare-Earth” Formulated Particles. J X-ray Sci Technol. 2011; 19:521–530.
85. Bedekar V, Dutta DP, Mohapatra M, Godbole SV, Ghildiyal R, Tyagi AK. Rare-Earth Doped Gadolinia Based Phosphors for Potential Multicolor and White Light Emitting Deep UV LEDs. Nanotechnology. 2009; 20:125707. [PubMed: 19420484]
86. Bulin AL, Truillett C, Chouikrat R, Lux F, Frochot C, Amans D, Ledoux G, Tillement O, Perriat P, Barberi-Heyob M, Dujardin C. X-Ray-Induced Singlet Oxygen Activation with Nanoscintillator-Coupled Porphyrins. J Phys Chem C. 2013; 117:21583–21589.
87. Kascakova S, Giuliani A, Lacerda S, Pallier A, Mercere P, Toth E, Refregiers M. X-Ray-Induced Radiophotodynamic Therapy (RPDT) Using Lanthanide Micelles: Beyond Depth Limitations. Nano Res. 2015; 8:2373–2379.
88. Wagstaff KM, Jans DA. Nuclear Drug Delivery to Target Tumour Cells. Eur J Pharmacol. 2009; 625:174–180. [PubMed: 19836384]
89. Rosenkranz AA, Jans DA, Sobolev AS. Targeted Intracellular Delivery of Photosensitizers to Enhance Photodynamic Efficiency. Immunol Cell Biol. 2000; 78:452–464. [PubMed: 10947873]
90. Mettath S, Munson BR, Pandey RK. DNA Interaction and Photocleavage Properties of Porphyrins Containing Cationic Substituents at the Peripheral Position. Bioconjugate Chem. 1999; 10:94–102.
91. Tada-Oikawa S, Oikawa S, Hirayama J, Hirakawa K, Kawanishi S. DNA Damage and Apoptosis Induced by Photosensitization of 5,10,15,20-Tetrakis (N-Methyl-4-Pyridyl)-21H,23H-Porphyrin *via* Singlet Oxygen Generation. Photochem Photobiol. 2009; 85:1391–1399. [PubMed: 19656322]
92. Moan J. On the Diffusion Length of Singlet Oxygen in Cells and Tissues. J Photochem Photobiol B. 1990; 6:343–347.
93. Schneider R, Tirand L, Frochot C, Vanderesse R, Thomas N, Gravier J, Guillemin F, Barberi-Heyob M. Recent Improvements in the Use of Synthetic Peptides for a Selective Photodynamic Therapy. Anticancer Agents Med Chem. 2006; 6:469–488. [PubMed: 17017856]

94. Akhlynina TV, Jans DA, Rosenkranz AA, Statsyuk NV, Balashova IY, Toth G, Pavo I, Rubin AB, Sobolev AS. Nuclear Targeting of Chlorin e6 Enhances Its Photosensitizing Activity. J Biol Chem. 1997; 272:20328–20331. [PubMed: 9252335]

95. Sheldon K, Liu D, Ferguson J, Gariepy J. Loligomers: Design of de novo Peptide-Based Intracellular Vehicles. Proc Natl Acad Sci U S A. 1995; 92:2056–2060. [PubMed: 7892224]

96. Dozzo P, Koo MS, Berger S, Forte TM, Kahl SB. Synthesis, Characterization, and Plasma Lipoprotein Association of a Nucleus-Targeted Boronated Porphyrin. J Med Chem. 2005; 48:357–359. [PubMed: 15658849]

97. Scaffidi JP, Gregas MK, Lauly B, Zhang Y, Vo-Dinh T. Activity of Psoralen-Functionalized Nanoscintillators against Cancer Cells Upon X-Ray Excitation. ACS Nano. 2011; 5:4679–4687. [PubMed: 21553850]

98. Deans AJ, West SC. DNA Interstrand Crosslink Repair and Cancer. Nat Rev Cancer. 2011; 11:467–480. [PubMed: 21701511]

99. Santamaria AB, Davis DW, Nghiem DX, McConkey DJ, Ullrich SE, Kapoor M, Lozano G, Ananthaswamy HN. P53 and Fas Ligand Are Required for Psoralen and UVA-Induced Apoptosis in Mouse Epidermal Cells. Cell Death Differ. 2002; 9:549–560. [PubMed: 11973613]

100. Derheimer FA, Hicks JK, Paulsen MT, Canman CE, Ljungman M. Psoralen-Induced DNA Interstrand Cross-Links Block Transcription and Induce P53 in an Ataxia-Telangiectasia and Rad3-Related-Dependent Manner. Mol Pharmacol. 2009; 75:599–607. [PubMed: 19064630]

101. Chen H, Wang GD, Chuang YJ, Zhen Z, Chen X, Biddinger P, Hao Z, Liu F, Shen B, Pan Z, Xie J. Nanoscintillator-Mediated X-Ray Inducible Photodynamic Therapy for *in Vivo* Cancer Treatment. Nano Lett. 2015; 15:2249–2256. [PubMed: 25756781]

102. Zhang C, Zhao K, Bu W, Ni D, Liu Y, Feng J, Shi J. Marriage of Scintillator and Semiconductor for Synchronous Radiotherapy and Deep Photodynamic Therapy with Diminished Oxygen Dependence. Angew Chem Int Ed Engl. 2015; 54:1770–1774. [PubMed: 25483028]

103. Clement S, Deng W, Drozdowicz-Tomsia K, Liu DM, Zachreson C, Goldys EM Bright. Water-Soluble CeF_3 Photo-, Cathodo-, and X-Ray Luminescent Nanoparticles. J Nanopart Res. 2015; 17

104. Clement S, Deng W, Camilleri E, Wilson BC, Goldys EM. X-Ray Induced Singlet Oxygen Generation by Nanoparticle-Photosensitizer Conjugates for Photodynamic Therapy: Determination of Singlet Oxygen Quantum Yield. Sci Rep. 2016; 6:19954. [PubMed: 26818819]

105. Zhang Y, Chen W, Wang S, Liu Y, Pope C. Phototoxicity of Zinc Oxide Nanoparticle Conjugatesin Human Ovarian Cancer Nih: Ovcar-3 Cells. J Biomed Nanotechnol. 2008; 4:432–438.

106. Liu YF, Zhang YB, Wang SP, Pope C, Chen W. Optical Behaviors of ZnO-Porphyrin Conjugates and Their Potential Applications for Cancer Treatment. Appl Phys Lett. 2008; 92:143901.

107. Generalov R, Kuan WB, Chen W, Kristensen S, Juzenas P. Radiosensitizing Effect of Zinc Oxide and Silica Nanocomposites on Cancer Cells. Colloids Surf, B. 2015; 129:79–86.

108. Staedler D, Magouroux T, Hadji R, Joulaud C, Extermann J, Schwung S, Passemard S, Kasparian C, Clarke G, Gerrmann M, Le Dantec R, Mugnier Y, Rytz D, Ciepielewski D, Galez C, Gerber-Lemaire S, Juillerat-Jeanneret L, Bonacina L, Wolf JP. Harmonic Nanocrystals for Biolabeling: A Survey of Optical Properties and Biocompatibility. ACS Nano. 2012; 6:2542–2549. [PubMed: 22324660]

109. Ma L, Zou XJ, Bui B, Chen W, Song KH, Solberg T. X-Ray Excited ZnS:Cu,Co Afterglow Nanoparticles for Photodynamic Activation. Appl Phys Lett. 2014; 105:013702.

110. Homayoni H, Jiang K, Zou X, Hossu M, Rashidi LH, Chen W. Enhancement of Protoporphyrin IX Performance in Aqueous Solutions for Photodynamic Therapy. Photodiagn Photodyn Ther. 2015; 12:258–266.

111. Rossi F, Bedogni E, Bigi F, Rimoldi T, Cristofolini L, Pinelli S, Alinovi R, Negri M, Dhanabalan SC, Attolini G, Fabbri F, Goldoni M, Mutti A, Benecchi G, Ghetti C, Iannotta S, Salviati G. Porphyrin Conjugated SiC/SiO_x Nanowires for X-Ray-Excited Photodynamic Therapy. Sci Rep. 2015; 5:7606. [PubMed: 25556299]

112. David Gara PM, Garabano NI, Llansola Portoles MJ, Moreno MS, Dodat D, Casas OR, Gonzalez MC, Kotler ML. ROS Enhancement by Silicon Nanoparticles in X-Ray Irradiated Aqueous Suspensions and in Glioma C6 Cells. J Nanopart Res. 2012; 14:1–13. [PubMed: 22448125]
113. Luksiene Z, Kalvelyte A, Supino R. On the Combination of Photodynamic Therapy with Ionizing Radiation. J Photochem Photobiol B. 1999; 52:35–42. [PubMed: 10643073]
114. Luksiene Z, Juzenas P, Moan J. Radiosensitization of Tumours by Porphyrins. Cancer Lett. 2006; 235:40–47. [PubMed: 15946797]
115. Takahashi J, Misawa M. Characterization of Reactive Oxygen Species Generated by Protoporphyrin IX under X-Ray Irradiation. Radiat Phys Chem. 2009; 78:889–898.
116. Bakalova R, Ohba H, Zhelev Z, Ishikawa M, Baba Y. Quantum Dots as Photosensitizers? Nat Biotechnol. 2004; 22:1360–1361. [PubMed: 15529155]
117. Samia AC, Chen X, Burda C. Semiconductor Quantum Dots for Photodynamic Therapy. J Am Chem Soc. 2003; 125:15736–15737. [PubMed: 14677951]
118. Kang Z, Zhang Y, Menkara H, Wagner BK, Summers CJ, Lawrence W, Nagarkar V. CdTe Quantum Dots and Polymer Nanocomposites for X-Ray Scintillation and Imaging. Appl Phys Lett. 2011; 98:181914. [PubMed: 21629562]
119. Letant SE, Wang TF. Semiconductor Quantum Dot Scintillation under Gamma-Ray Irradiation. Nano Lett. 2006; 6:2877–2880. [PubMed: 17163723]
120. Takahashi J, Misawa M. Analysis of Potential Radiosensitizing Materials for X-Ray-Induced Photodynamic Therapy. Nanobiotechnology. 2008; 3:116–126.
121. Yang W, Read PW, Mi J, Baisden JM, Reardon KA, Larner JM, Helmke BP, Sheng K. Semiconductor Nanoparticles as Energy Mediators for Photosensitizer-Enhanced Radiotherapy. Int J Radiat Oncol Biol Phys. 2008; 72:633–635. [PubMed: 19014777]
122. Das, S.; Thorek, DLJ.; Grimm, J. Chapter Six - Cerenkov Imaging. In: Martin, GP.; Paul, BF., editors. Adv Cancer Res. Vol. 124. Academic Press; 2014. p. 213-234.
123. Spinelli AE, Boschi F. Novel Biomedical Applications of Cerenkov Radiation and Radioluminescence Imaging. Physica Medica. 2015; 31:120–129. [PubMed: 25555905]
124. Thorek D, Robertson R, Bacchus WA, Hahn J, Rothberg J, Beattie BJ, Grimm J. Cerenkov Imaging - a New Modality for Molecular Imaging. Am J Nucl Med Mol Imaging. 2012; 2:163–173. [PubMed: 23133811]
125. Tanha K, Pashazadeh AM, Pogue BW. Review of Biomedical Cerenkov Luminescence Imaging Applications. Biomed Opt Express. 2015; 6:3053–3065. [PubMed: 26309766]
126. Mitchell GS, Gill RK, Boucher DL, Li C, Cherry SR. *In Vivo* Cerenkov Luminescence Imaging: A New Tool for Molecular Imaging. Philos Trans R Soc A. 2011; 369:4605–4619.
127. Dothager RS, Goiffon RJ, Jackson E, Harpstrite S, Piwnica-Worms D. Cerenkov Radiation Energy Transfer (CRET) Imaging: A Novel Method for Optical Imaging of PET Isotopes in Biological Systems. PLoS One. 2010; 5:e13300. [PubMed: 20949021]
128. Liu H, Zhang X, Xing B, Han P, Gambhir SS, Cheng Z. Radiation-Luminescence-Excited Quantum Dots for *in Vivo* Multiplexed Optical Imaging. Small. 2010; 6:1087–1091. [PubMed: 20473988]
129. Volotskova O, Sun C, Stafford JH, Koh AL, Ma X, Cheng Z, Cui B, Pratx G, Xing L. Efficient Radioisotope Energy Transfer by Gold Nanoclusters for Molecular Imaging. Small. 2015; 11:4002–4008. [PubMed: 25973916]
130. Hu Z, Qu Y, Wang K, Zhang X, Zha J, Song T, Bao C, Liu H, Wang Z, Wang J, Liu Z, Liu H, Tian J. *In Vivo* Nanoparticle-Mediated Radiopharmaceutical-Excited Fluorescence Molecular Imaging. Nat Commun. 2015; 6:7560. [PubMed: 26123615]
131. Cao X, Chen X, Kang F, Zhan Y, Cao X, Wang J, Liang J, Tian J. Intensity Enhanced Cerenkov Luminescence Imaging Using Terbium-Doped Gd_2O_2S Microparticles. ACS Appl Mater Interfaces. 2015; 7:11775–11782. [PubMed: 25992597]
132. Tian Y, Cao WH, Luo XX, Fu Y. Preparation and Luminescence Property of Gd_2O_2S: Tb X-Ray Nano-Phosphors Using the Complex Precipitation Method. J Alloys Compd. 2007; 433:313–317.
133. Carel, WEvE. Inorganic Scintillators in Medical Imaging. Phys Med Biol. 2002; 47:R85–106. [PubMed: 12030568]

134. Retif P, Pinel S, Toussaint M, Frochot C, Chouikrat R, Bastogne T, Barberi-Heyob M. Nanoparticles for Radiation Therapy Enhancement: The Key Parameters. Theranostics. 2015; 5:1030–1044. [PubMed: 26155318]

135. Zhang JZ. Ultrafast Studies of Electron Dynamics in Semiconductor and Metal Colloidal Nanoparticles: Effects of Size and Surface. Acc Chem Res. 1997; 30:423–429.

136. Hardman R. A Toxicologic Review of Quantum Dots: Toxicity Depends on Physicochemical and Environmental Factors. Environ Health Perspect. 2006; 114:165–172. [PubMed: 16451849]

137. Pagano G, Guida M, Tommasi F, Oral R. Health Effects and Toxicity Mechanisms of Rare Earth Elements-Knowledge Gaps and Research Prospects. Ecotoxicol Environ Saf. 2015; 115:40–48. [PubMed: 25679485]

138. Antonietta Zoroddu M, Medici S, Ledda A, Marina Nurchi VI, Lachowicz J, Peana M. Toxicity of Nanoparticles. Curr Med Chem. 2014; 21:3837–3853. [PubMed: 25306903]

139. Amir Ata S, Morteza M. Toxicity of Nanoparticles in Nanoparticles for Biotherapeutic Delivery. Future Med. 2015; 1:112–131.

140. Neri D, Bicknell R. Tumour Vascular Targeting. Nat Rev Cancer. 2005; 5:436–446. [PubMed: 15928674]

141. Murphy EA, Majeti BK, Barnes LA, Makale M, Weis SM, Lutu-Fuga K, Wrasidlo W, Cheresh DA. Nanoparticle-Mediated Drug Delivery to Tumor Vasculature Suppresses Metastasis. Proc Natl Acad Sci U S A. 2008; 105:9343–9348. [PubMed: 18607000]

142. Zhen Z, Tang W, Chuang YJ, Todd T, Zhang W, Lin X, Niu G, Liu G, Wang L, Pan Z, Chen X, Xie J. Tumor Vasculature Targeted Photodynamic Therapy for Enhanced Delivery of Nanoparticles. ACS Nano. 2014; 8:6004–6013. [PubMed: 24806291]

143. Shi S, Yang K, Hong H, Valdovinos HF, Nayak TR, Zhang Y, Theuer CP, Barnhart TE, Liu Z, Cai W. Tumor Vasculature Targeting and Imaging in Living Mice with Reduced Graphene Oxide. Biomaterials. 2013; 34:3002–3009. [PubMed: 23374706]

144. Chen F, Cai W. Tumor Vasculature Targeting: A Generally Applicable Approach for Functionalized Nanomaterials. Small. 2014; 10:1887–1893. [PubMed: 24591109]

145. Liu X, Li H, Chen Y, Jin Q, Ren K, Ji J. Mixed-Charge Nanoparticles for Long Circulation, Low Reticuloendothelial System Clearance, and High Tumor Accumulation. Adv Healthcare Mater. 2014; 3:1439–1447.

146. Fan W, Shen B, Bu W, Chen F, He Q, Zhao K, Zhang S, Zhou L, Peng W, Xiao Q, Ni D, Liu J, Shi J. A Smart Upconversion-Based Mesoporous Silica Nanotheranostic System for Synergetic Chemo-/Radio-/Photodynamic Therapy and Simultaneous MR/UCL Imaging. Biomaterials. 2014; 35:8992–9002. [PubMed: 25103233]

147. Thomas B. IMRT: A Review and Preview. Phys Med Biol. 2006; 51:R363–R379. [PubMed: 16790913]

148. Mackie TR, Holmes T, Swerdloff S, Reckwerdt P, Deasy JO, Yang J, Paliwal B, Kinsella T. Tomotherapy: A New Concept for the Delivery of Dynamic Conformal Radiotherapy. Med Phys. 1993; 20:1709–1719. [PubMed: 8309444]

149. Jeraj R, Mackie TR, Balog J, Olivera G, Pearson D, Kapatoes J, Ruchala K, Reckwerdt P. Radiation Characteristics of Helical Tomotherapy. Med Phys. 2004; 31:396–404. [PubMed: 15000626]

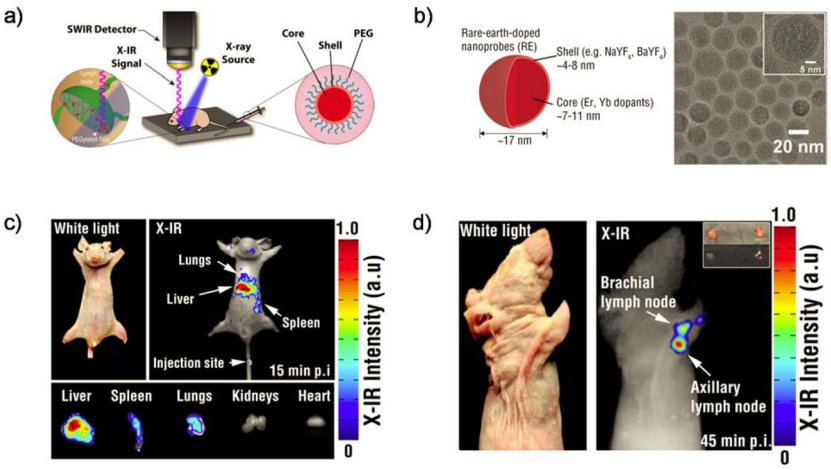

Figure 1.

(**a**) Schematic of REs showing the lanthanide-doped core surrounded by an undoped shell. (**b**) TEM images of REs reveal spherical morphology. (**c**) Nanoprobe clearance visualized in mice 15 min post injection using X-IR imaging. (**d**) X-IR imaging of axillary and brachial lymph nodes. Reproduced with permission from [65]. Copyright 2015 American Chemical Society.

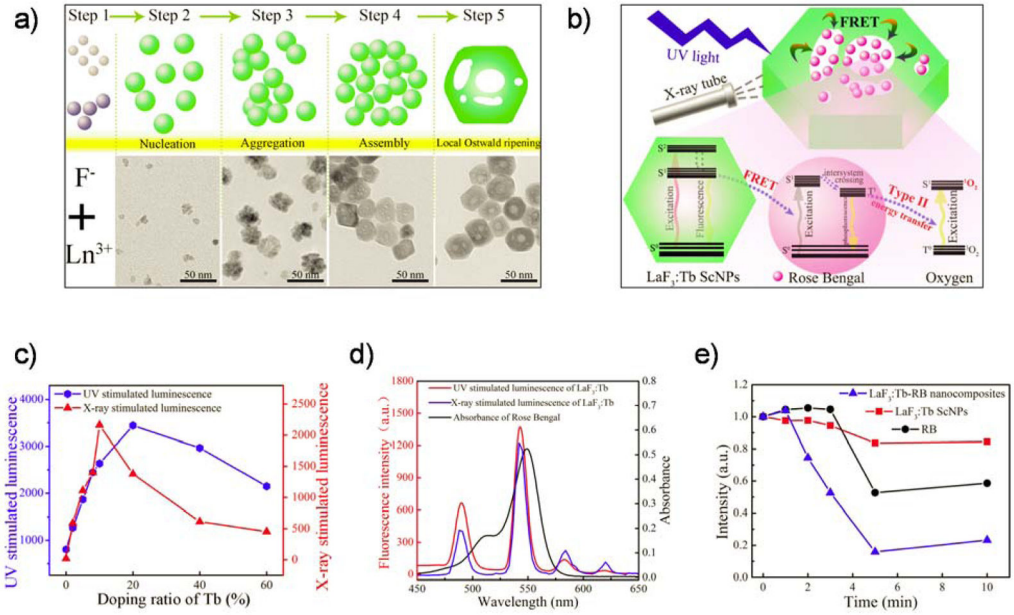

Figure 2.

(**a**) A proposed formation mechanism of mesoporous $LaF_3:Tb^{3+}$ nanoparticles. (**b**) Schematic represents mesoporous $LaF_3:Tb^{3+}$-RB nanocomposites and their potential application in deep PDT. (**c**) Luminescence intensity at 544 nm under UV and X-ray stimulation of mesoporous $LaF_3:Tb^{3+}$ ScNPs with varied Tb^{3+} doping ratios. (**d**) Spectrum overlap between luminescence of $LaF_3:Tb^{3+}$ ScNPs and absorption of RB. (**e**) Decrease of emission intensity of 1,3-diphenylisobenzofuran treated with $LaF_3:Tb^{3+}$ ScNPs, RB, and LaF_3:Tb-RB nanocomposites, respectively, after different irradiation times. Reproduced with permission from [82]. Copyright 2015 American Chemical Society.

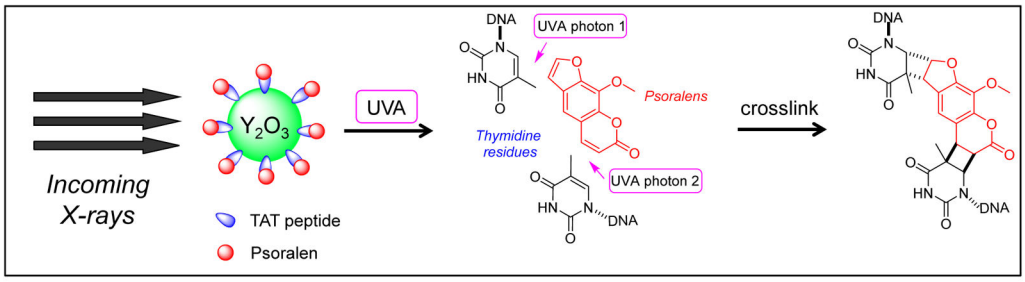

Figure 3.

Schematic representing the mechanism of a Y_2O_3 nanosystem with induced DNA cross-linking upon X-ray irradiation.

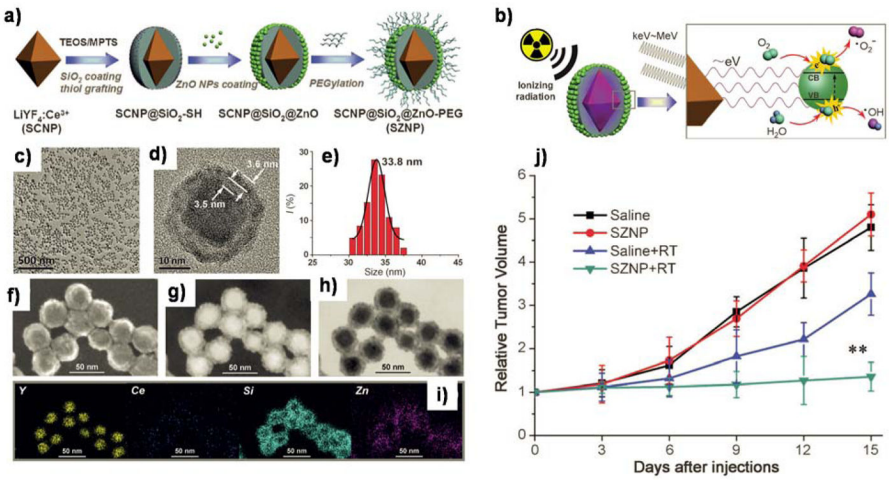

Figure 4.

(**a**) A schematic illustration of the synthetic route to monodisperse SZNPs and (**b**) the mechanism of ionizing radiation-induced photodynamic therapy. TEM images at (**c**) low and (**d**) high magnifications, and (**e**) the corresponding size distribution of SZNPs. STEM image of SZNPs using (**f**) SEM, (**g**) dark-field, and (**h**) bright-field modes. (**i**) Corresponding element mappings of SZNPs. (**j**) *In vivo* ionizing-radiation-induced SZNPs-mediated synchronous radiotherapy and PDT. Reproduced with permission from [102]. Copyright 2015 WILEY-VCH Verlag GmbH & Co. KGaA, Weinheim.

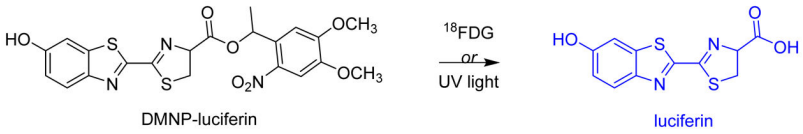

Figure 5.

Uncaging reaction of DMNP-luciferin. Luciferin can be released from DMNP-luciferin by irradiation with UV 365 nm or with radiation luminescence generated from ^{18}FDG.

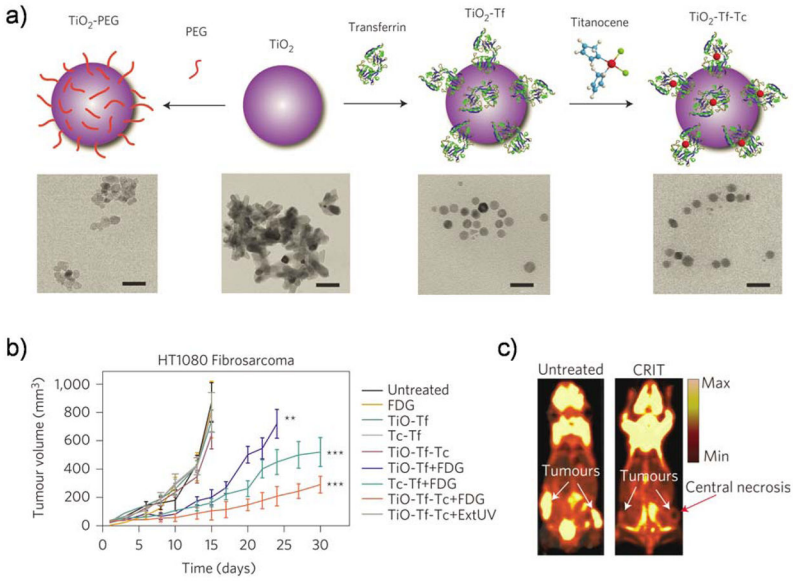

Figure 6.

(**a**) A schematic illustrating the synthesis of TiO_2-PEG, TiO_2-Tf and TiO_2-Tf-Tc. Below (left to right) are the TEM images of TiO_2-PEG, TiO_2 aggregates, TiO_2-Tf and TiO_2-Tf-Tc (right). (**b**) *In vivo* Cerenkov radiation-induced therapy (CRIT) through a one-time systemic administration of the constructs and ^{18}FDG in HT1080-tumor-bearing Athymic nu/nu mice. (**c**) FDG-PET images of an untreated (left) mouse (15 days) with bilateral HT1080 tumors and after CRIT (30 days) (right). Reproduced with permission from [76]. Copyright 2015 Nature Publishing Group.

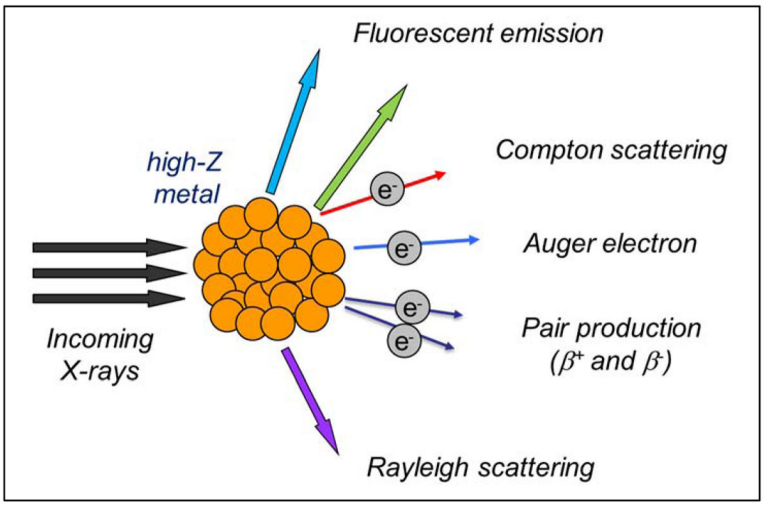

Scheme 1.

A diagram demonstrating the outcomes when X-rays hit a high-Z substance.

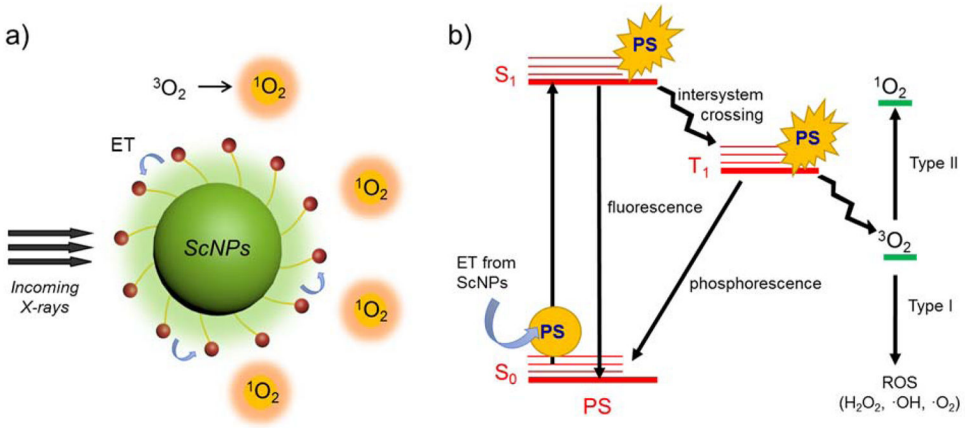

Scheme 2.

The principle of X-ray activatable nanoparticles for PDT. (**a**) Schematic represents scintillating nanoparticles (ScNPs) that act as an X-ray transducer to generate $^1O_2$ through the energy transfer (ET) process. (**b**) Diagram represents the PDT mechanism that occurs when energy is transferred from ScNPs to activate the PS. The PS's electrons from the ground state (S_0) will absorb energy and move to singlet-excited states (S_1). Some of the absorbed energy will be released *via* intersystem crossing (ISC), and the promoted electron will move to a triplet-excited state (T_1). This triplet state has a relatively long half-life, allowing energy to be transferred to nearby oxygen molecules. This generates $^1O_2$ in most cases *via* the type II pathway, which can damage the cells in the surrounding area.

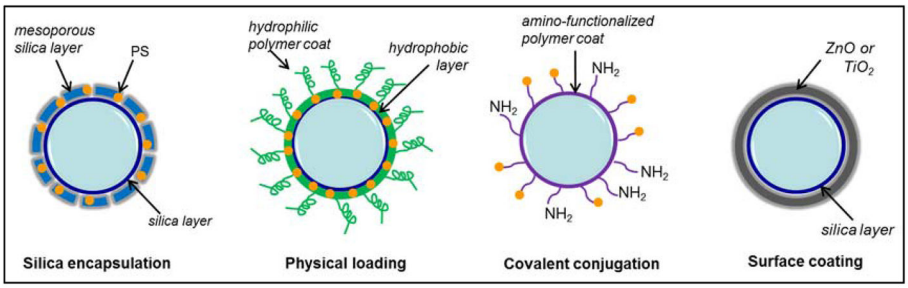

Scheme 3.
Schematic depicting different PS loading strategies.

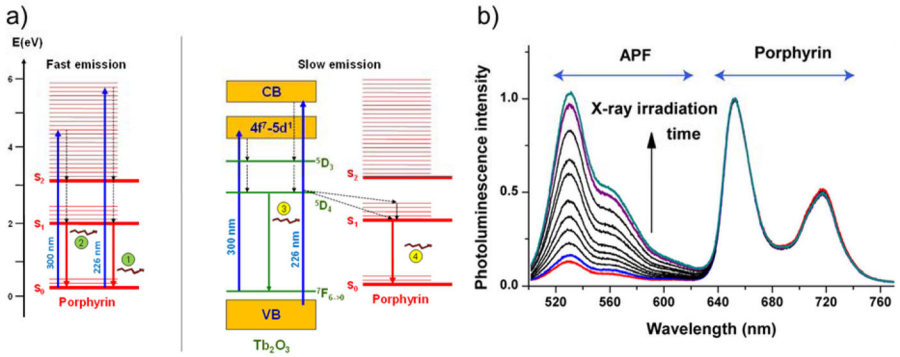

Scheme 4.

(**a**) (Left) Direct excitation of porphyrin by 226 or 300 nm lasers. Porphyrin is excited to high vibrational energy levels and relaxes in a non-radiative decay to the S_2 then S_1 level. Relaxation from S_1 to S_0 results in visible emissions 1 and 2. (Right) Indirect excitation of porphyrin. Tb_2O_3@SiO_2 absorbs energy from light at 226 or 300 nm and is then excited to higher energy levels. Once nonradiative decays to $^5D_4$ level, Tb can either emit visible light 3 or transfer energy to porphyrin to emit red light 4. (**b**) Emission spectra measured under a 490 nm diode excitation after increasing X-ray irradiation time. The Tb_2O_3@SiO_2 grafted TPP is more efficient in generating ROS that oxidize APF under X-ray irradiation than porphyrin solution. Reproduced with permission from [86]. Copyright 2013 American Chemical Society.

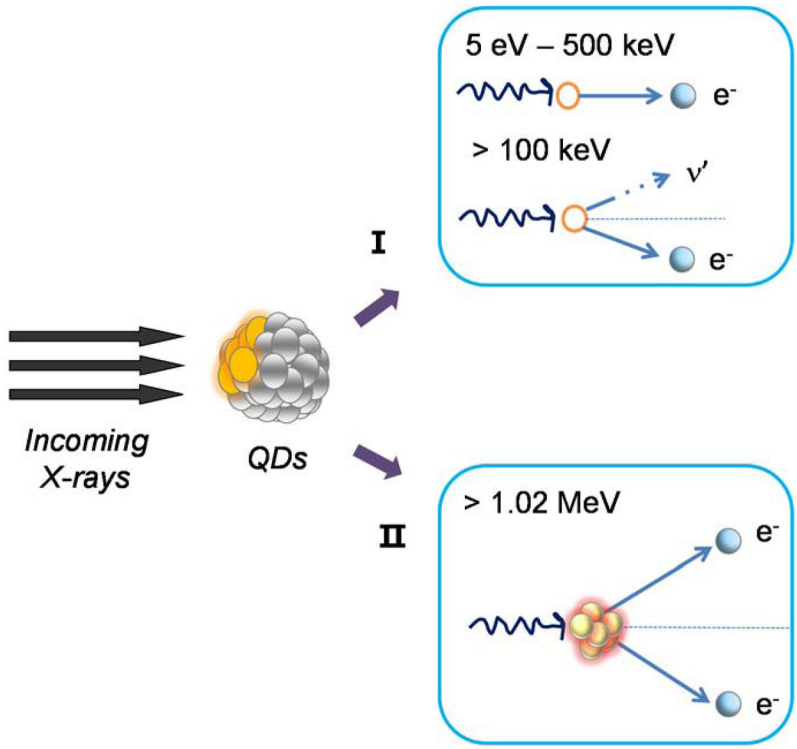

Scheme 5.

A schematic presenting the possible situation of when a high-energy photon (X-rays or γ-rays) hits QDs: (I) a high speed electron was released from a QD due to photon energy transfer to the electron (photoelectric ionization effect) or Compton scattering, where the incident photon continues scattering its travel with lower energy until the (II) photon annihilation on a nucleus of an atom and generation of an electron-positron pair. The positron will annihilate on a nucleus of an atom to generate an electron-positron pair with two 0.51 MeV photons. These particles will further lose their energy through the photoelectric effect or Compton scattering. Electrons generated in the incidents (I) and (II) will induce secondary high-speed electrons as well as Auger electrons. Such electrons that can escape into the environment will be captured by an acceptor (*i.e.* water, biomolecule, oxygen, nitrogen oxides), which localizes near the QDs and induces biomolecular radicals, superoxide, hydroxyl radicals, peroxynitrite anions, or nitric oxide radicals.

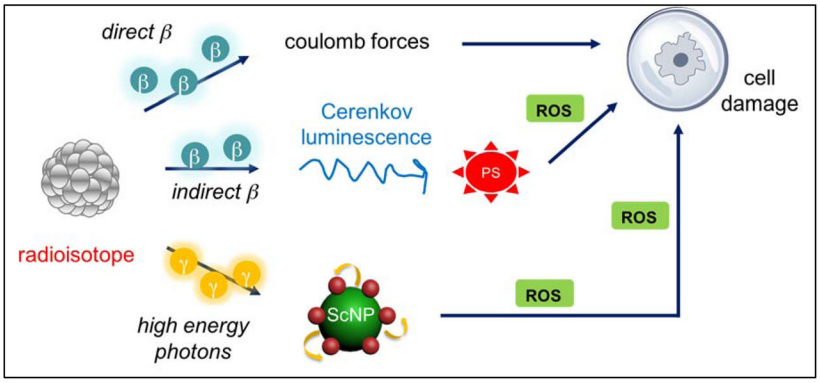

Scheme 6.

Schematic illustration of radioisotope energy transfer processes. Radioisotopes can emit Cerenkov radiation to directly activate photosensitizers that can absorb light in the 200–500 nm range. Some radioisotopes can generate high energy photons, such as γ-radiation, that can be absorbed by certain types of nanoparticles (*i.e.* scintillating nanoparticles, ScNPs). In this case, the photosensitizers will be indirectly excited by the radionuclide. Once the PS is activated, ROS will be generated to damage the surrounding cell/tissue.

Table 1

X-ray scintillators for cancer therapy

Nanosystem	Size	PS	Attachment Strategy	X-ray doses	Biological Experiment	Ref.
$SrAl_2O_4:Eu^{2+}$	80 nm	MC540	Pore loading	0.5 Gy	U87MG xenograft (it.)	101
$LaF_3:Tb^{3+}$	15 nm	MTCP	Covalent binding	120 keV	N/A	80
LaF_3:Tb	3–45 nm	RB	Covalent binding	2–10 keV	N/A	82
LaF_3:Tb	3–45 nm	RB	Covalent binding	N/A	Tumor model (it.)	83
$LaF_3:Ce^{3+}$	2 μm	PPIX	Physical loading	3 Gy	PC3 cells	73
CeF_3	7–11 nm	VP	Physical loading	6 Gy, 8 keV or 6 MeV	Panc-1	104
Tb_2O_3	10 nm	porphyrin	Covalent binding	N/A	N/A	86
Y_2O_3	12 nm	psoralen	Covalent binding	2 Gy, 160 or 320 kVp	PC3 cells	97
ZnS:Cu,Co	4 nm	TBrRh123	Covalent binding	2 Gy	PC3 cells	109
APTES	N/A	PPIX	Coating	8 Gy	PC3 cells	110
$LiYF_4:Ce^{3+}$	34 nm	ZnO	Coating	8 Gy	HeLa cells	102
Gd_2O_2S:Tb	20 μm	Photofrin II	Co-location	120keV, 20 mAs	human glioblastoma cells	84
SiC/SiO_x NWs	20 nm	porphyrin	Covalent binding	2 Gy, 6 MV	A549 cells	111
ZnO/SiO_2	98 nm	ZnO	Coating	200 kVp, 2 Gy	LNCaP and Du145 cells	107
GdEuC12 micelle	4.6 nm	Hyp	Physical loading	400 mA	HeLa cells	87
Cu-Cy	50–100 nm	self	No PS	5 Gy	MCF-7 xenograft (it.)	73

it. = intratumoral injection, N/A = not available